# 修 士 論 文 の 和 文 要 旨

| 研究科・専攻 | 大学院　情報理工学研究科　情報・ネットワーク工学専攻　博士前期課程 | | |
|---|---|---|---|
| 氏　　名 | 廣澤 直也 | 学籍番号 | 1931124 |
| 論 文 題 目 | 環境発電を用いた多元接続通信における<br>情報鮮度最小化のための最適送信法に関する研究 | | |


要 旨

エナジーハーベスティング (EH: Energy Harvesting) 電源を具備した複数のセンサーノード (SN: Sensor Node) が，共通の 1 台のフュージョンセンターと通信を行う多元接続方式について，情報鮮度 (AoI: Age of Information) を評価指標として議論する．具体的には，時分割多元接続方式 (TDMA: Time-Division Multiple Access)，周波数分割多元接続方式 (FDMA: Frequency-Division Multiple Access)，そしてスロット化アロハの 3 つの方式を想定する．特に 2 つのグラントアクセス，TDMA と FDMA の場合には，AoI の凸性を利用し AoI を最小にするための凸最適化問題を定義する．定義する最適化問題に対し，TDMA では観測情報を送信する準備が整った SN から順番に送信する貪欲アルゴリズムを適用し，FDMA では，交互方向乗数法，および二分探索法を用いて，最小 AoI を導出する．一方，SN の送信すべきデータ量が少ない場合には，無線資源割り当てに必要なオーバヘッドが無視できず，排他的な割り当てを行う必要のないグラントフリーアクセスがグラントアクセスと比較して有利となる場合がある．そこで，グラントフリーアクセスの 1 つであるスロット化アロハの AoI を TDMA，FDMA とは異なる形で定式化するとともに，EH を考慮した場合のデータ伝送処理についても言及する．数値結果では，TDMA と FDMA それぞれの場合について，各 SN に送信時間，周波数帯域割り当てを行うための最適化問題を解き，2 つのグラントアクセスの AoI を比較する．さらに，スロット化アロハが達成可能な AoI を示し，オーバヘッドを考慮した TDMA と比較することで，オーバヘッドと送信時間スロットの割合に対し，ランダムアクセスがより小さい AoI を達成する領域を明らかにする．

令和2年度　修士論文

# Transmission Strategy for Minimum Age of Information over Energy Harvesting Multiple-Access Channels

# 環境発電を用いた多元接続通信における情報鮮度最小化のための最適送信法に関する研究


学籍番号　1931124

氏　　名　廣澤 直也

指導教員　石橋　功至 准教授

電気通信大学　情報理工学研究科

情報・ネットワーク工学専攻


提出日　令和3年1月25日

# Transmission Strategy for Minimum Age of Information over Energy Harvesting Multiple-Access Channels

**Naoya Hirosawa**

Department of Computer and Network Engineering
The University of Electro-Communications

This thesis is submitted for the degree of
*Master in Engineering*

March 2021

# Acknowledgements

This thesis is a summary of my studies in the master's program at the University of Electro-Communications, Tokyo, Japan. I would like to express my sincere gratitude to everyone who has supported me, especially my supervisor, Associate Professor Koji Ishibashi, for his constructive suggestions and thoughful guidance. Moreover, Hiroki Iimori, who is Ph. D student of Jacobs University, Bremen, and Prof. Dr. Giuseppe Thadeu Freitas de Abreu, who is Prof. of Jacobs University, Bremen, encouraged me to pursue my research interest though valuable advices and discussions. Moreover, I would like to thank Prof. Yasushi Yamao, Takeo Fujii, and Associate Prof. Koichi Adachi for their insightful advice. I am also grateful to all the member of Advanced Wireless & Communication Research (AWCC) center. Finally, I would like to sincerely thank my family, Keiichi, Noriko, and Fumiya.

Naoya Hirosawa
January 25th, 2021

# Abstract

We consider an energy harvesting wireless sensor network (EH-WSN) where single-antenna sensors communicate with a common fusion center (FC) with the aim of cooperatively minimizing the overall average age of information (AoI). Specifically, we propose new resource allocation algorithms to minimize the average AoI in an EH-WSN employing common multiple-user schemes, in particular time-division multiple access (TDMA), frequency-division multiple access (FDMA) and slotted ALOHA. To this end, we take advantage of the convexity of the derived AoI, enabling an optimal resource block assignment, implemented as a greedy algorithm for TDMA systems and in the form of an alternating direction method of multipliers (ADMM) scheme for FDMA systems. The optimality of the greedy resource allocation scheme derived for the TDMA case is obtained by design, whereas that of the ADMM-based method derived for the FDMA case is demonstrated numerically. Furthermore, for slotted ALOHA, we discuss the formulation of AoI and introduce the transmission model, and compared it to grant access schemes with the overhead. Simulation results indicate that the choice between TDMA, FDMA or slotted ALOHA depends on the available resources, size of the data packet, cost of overhead and the time of packet observation in the system.

# Table of contents

# List of figures

# Chapter 1

# Introduction

Owing to the latest advances in sensing and data transmission technologies, various monitoring services employing wireless sensor networks (WSNs) have been proposed over the years to solve problems in domains such as transportation [1], health [2], and the environment [3], culminating with the notion of digital twins (DTs) [4, 5].

Digital twins are digital representations of physical devices or systems based on data collected in real-time, which continuously track physical changes in the devices/systems while forecasting possible future states of the corresponding physical components. Given that a very large number of devices may be connected to feed a DT, the corresponding data must be collected in a distributed and reliable fashion. The current sensors using primary or secondary batteries cannot meet these requirements because of the huge maintenance cost that is incurred as the number of sensors increases. Therefore, there are high demands on energy harvesting (EH) WSNs, well known for their self-reliance and low-maintenance characteristics.

Indeed, EH techniques have been well-studied [6–11] and matured enough that it can be assumed that the technology will soon become ubiquitous, equipping devices with the capability to convert energy from natural (*i.e.* solar radiation, vibration, and temperature differences) or artificial (*i.e.* wireless energy transfer) sources into electric power required to run sensors. Besides, as shown in the example in Fig. 1.1, SN equipped with EH can be created or purchased easier. Moreover, the networking protocols specific for EH-WSNs using these SNs have also been developed [12–18], and practical applications have been advanced.

However, a problem associated with the latter paradigm that has received comparatively less attention is the "*freshness*" issue or the age of information (AoI) of messages collected and distributed by EH-WSNs. Indeed, protocols for EH-WSNs have so far largely focused on energy and data arrival processes, without addressing the fact that, in practice, data collected by EH-WSNs may be outdated, which affects their suitability to DT applications. Thus, a new

concept is needed to ensure the freshness of information in such time-bound data-oriented systems, as argued *e.g.* in [19, 20].

As noted in [19, 20], AoI can be defined as the time elapsed from the moment the information is generated and captured by the sensor, until it is received by the destination, which, in the case of our application of interest can be considered as the FC. Interestingly, as reported in [21–25], the optimal strategy that minimizes AoI is different from conventional data rate maximization and delay minimization strategies, motivating the design of new WSN optimization approaches for DT applications in which freshness of information is fundamental.

However, similar to data rate and delay, AoI is also impacted by the presence of multiple users – or in the context of WSNs, multiple sensors – that compete for the same frequency and time resources, which must therefore be properly allocated or scheduled. Considering this issue, resource allocation schemes aimed at minimizing AoI in TDMA and frequency-division multiple access (FDMA) systems have been studied in [26–30]. In addition, the characterization of AoI has been studied for random access networks in [31] and for carrier sense multiple access (CSMA) networks with distributed scheduling in [32]. We remark, however, that the scenarios considered in the aforementioned works are not constrained by the possibility of battery outage or random energy arrival processes, as faced by maintenance-free EH-WSNs. In turn, EH-oriented AoI minimization problems have been previously investigated in [33–38], but for a unidirectional communication scenario in which a single EH-SN continuously sends status updates to a single FC.

Considering that practical DT-WSN scenarios rely on multiple SNs communicating with a common FC, we argue that in order to address the DT case, contributions such as those of [33–38] need to be generalized, in particular toward the design of optimal resource allocation handling multiple SNs, aimed at minimizing the average AoI under battery-constrained conditions. To the best of our knowledge, no mechanism to minimize the AoI in DT EH-WSNs has been proposed thus far. In this study, we therefore investigate a system with multiple EH-SNs that simultaneously communicates with a common FC, proposing novel resource allocation algorithms both in TDMA and FDMA modes to minimize the corresponding average aggregate AoI. In addition to the above, if the amount of data transmitted by the sensors is small, the overhead required to allocate resources cannot be ignored in grant access such as TDMA and FDMA. On the other hand, random access without resource allocation, namely grant-free access[39, 40], may achieve a smaller AoI than grant access since each SN transmits data autonomously and does not have any overhead. In [31], the AoI has been evaluated in grant-free access, however, there is no discussion comparing grant-free access with grant access and which can acieve a smaller AoI Therefore, in order

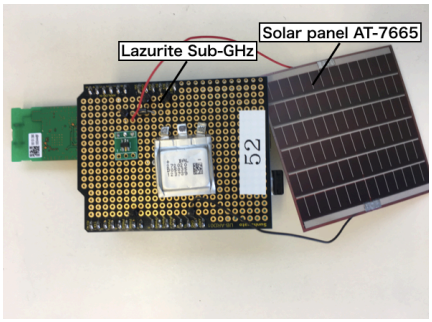


(a) Solar EH-SN [17]


(b) Vibration EH-SN [41]

Fig. 1.1 Example of EH-SNs

to compare grant access with grant-free access, one of the basic grant-free access, slotted ALOHA, is discussed and its AoI performance is clarified.

The remainder of this thesis is organized as follows. The system model is described in Chapter 2, while Chapter 3 provides the definition of the AoI for EH-WSN, its convexity analysis, and new radio resource allocation algorithms for both TDMA and FDMA scenarios. In Chapter 4, we investigate the AoI expression in the slotted ALOHA scheme and explain the process of slotted ALOHA with EH-SN. The numerical results of the proposed algorithms are shown in Chapter 5, and Chapter 6 concludes this thesis.

**Notation**

Vectors and scalars are denoted by bold and standard fonts, such as in $\mathbf{x}$ and $x$, respectively. Sets of natural, positive natural, real, positive real, and complex numbers are respectively denoted by $\mathbb{N}$, $\mathbb{Z}^+$, $\mathbb{R}$, $\mathbb{R}^+$ and $\mathbb{C}$. The absolute value and ceiling functions are respectively denoted by $|x|$ and $\lceil x \rceil \triangleq \min\{n \in \mathbb{Z} \,|\, n \geq x\}$. Finally, the fact that a random variable $x$ follows the complex Gaussian distribution with mean $\mu$ and variance $\sigma^2$ is expressed as $x \sim \mathscr{C}(\mu, \sigma^2)$.

# Chapter 2

# System Model

## 2.1 Energy-Harvesting Wireless Sensor Network

Consider the uplink of a WSN consisting of $N$ single-antenna SNs sending status updates to one common FC, as shown in Fig. 2.1, such that each SN is subjected to limited energy harvested from environmental sources such as solar radiation, vibration, and radio frequency waves. It is assumed that the length of an uplink packet transmitted by an $i$-th SN is denoted by $D_i$ [bits], where $i \in \{1,2,\ldots,N\}$ denotes the node index, and all the harvested energy (no loss) is stored in a supercapacitor embedded in each SN. For the sake of simplicity but without loss of generality, we assume that the initial amount of energy stored in each supercapacitor is 0 [J]. The amount of energy that can be harvested fluctuates with time as shown in Fig. 2.2, although it can be averaged by long-term observation because it is expressed as the sum of integrations over time. In this thesis, we assume that the average energy can be harvested as shown by the broken line in Fig. 2.2. From the above, we denote the average harvested power at the $i$-th SN by $E_i$ [W], the amount of energy available after $k_i \in \mathbb{Z}^+$ normalized unit time samples can be expressed as $k_i E_i$ [J]. Also we set $n_i \in \mathbb{Z}^+$ to be the time it consumed to complete the transmission so that, in Grant-Access scheme, the transmitted power is $k_i E_i / n_i$ [W]. For the sake of simplicity, it is assumed that all the harvested power will be consumed at transmission.

In turn, the communication channel from the $i$-th SN to the FC is modeled as a flat fading channel with gains $h_i$, subjected to zero-mean additive white Gaussian noise (AWGN) characterized by a noise power spectral density $N_0$ [W/Hz], with a total system bandwidth of $B_{\text{total}}$ [Hz].

In this thesis, three multiple access schemes such as TDMA, FDMA, and slotted ALOHA, are considered, and next each scheme is explained. In TDMA, in order to avoid the channel-overlap, each channel is divided in the time axis and assigned to each SN. In

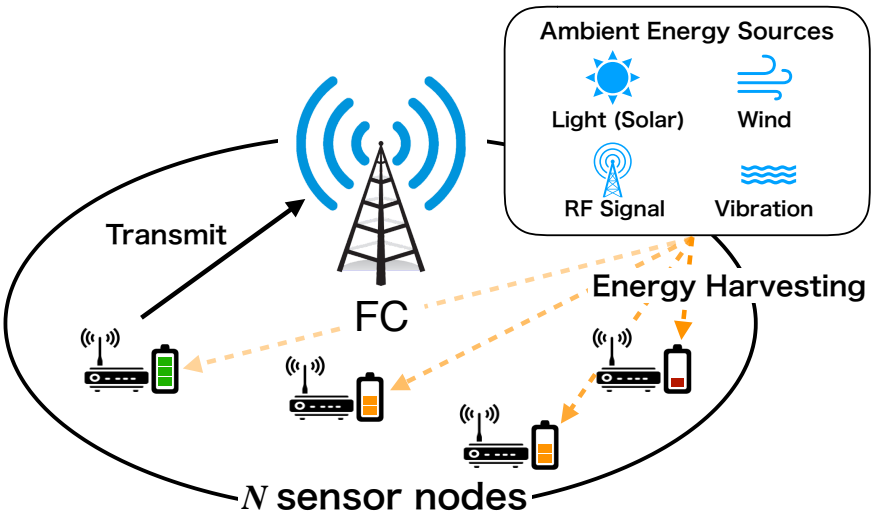


Fig. 2.1 EH-WSN with $N$ single-antenna EH-SN and a common FC.

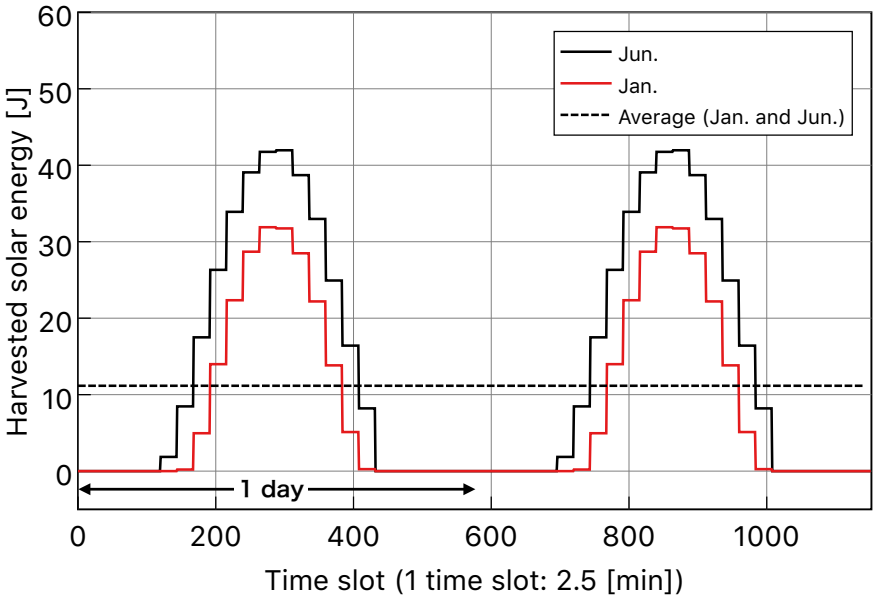


Fig. 2.2 Solar energy harvested by SN in each time slot relative to the solar irradiance in January and June for Delhi [42]. The black broken line shows the average harvested solar energy in January and June.

other words, each SN transmits the data *in order* by using the total bandwidth $B_{\text{total}}$ after harvesting enough energy. For the ease of the system model, the guard interval is not considered. The transmission order is determined by the *greedy* algorithm, which starts with the SN that can transmit the data a the earliest at each time-slot. This will be explained in detail in subsequent chapters.

In FDMA, the system bandwidth is divided so as nonoverlapping and each SN is assigned a different bandwidth. In contrast to TDMA, multiple SN can transmit data at the same time since each SN communicates with FC using different orthogonal bandwidth. As in TDMA, the guard band is not considered. TDMA and FDMA, which we will discuss next section, require overhead for resource allocation, but the cost of the overhead is assumed to be the same for both schemes and is not considered when comparing TDMA and FDMA.

In slotted ALOHA with EH, each SN operates based on [43] and the detail will be described in Chapter 4.

## 2.2 Model of Data Generation Time for AoI Evaluation

Another aspect of the system model that is fundamental to analyzing the AoI for a distributed system is the time-origin of the information relative to the timestamp of the transmitted packet. To elaborate, analyses of AoI can be found in the literature; they are based on two distinct timing conditions, namely, a *distributed* model in which each SN has its own time origin, as adopted *e.g.* [29], and a *concurrent* model in which a common time origin is shared by all SNs as adopted for instance in [30, 33]. A brief explanation of the two models is that the concurrent model generates data as soon as the system starts for all SNs (i.e., at t=0), while the distributed model generates data when the channel is assigned to communicate with the FC, for example, in the case of TDMA. As we will discuss in detail later, since the AoI is expressed in terms of the time elapsed from the data was generated, whether it is a concurrent or distributed model is very important in analyzing the AoI.

Both these models are valid as they address distinct applications. For example, the distributed model employed in [29] is better suited to applications such as the monitoring of structures (*e.g.* bridges, tunnels, and towers), in which multiple sensors are installed on the same structure, so that an update indicating a status deterioration at any of the SNs indicates a deterioration of the structure itself. In turn, the concurrent model adopted *e.g.* in [30, 33], which is also more commonly utilized, addresses applications such as DT, in which different pieces of information collected by different SNs contribute to composing a larger whole, *e.g.* the DT of a given system.

Having made this remark, in this thesis, we focus on the latter (more prevalent) concurrent timing approach, in which the multi-access scheme employed has also a greater impact, especially in the context of EH networks, as it affects both the time SNs must wait from the moment data is collected until they can transmit in the case of TDMA schemes, as well as the time available for EH nodes to gather sufficient energy to transmit, in the case of an FDMA scheme.

## 2.3 Chapter Summary

In this chapter, we introduced the system model of EH-WSN with some variables used in this thesis and also briefly described three multiple access schemes, TDMA, FDMA, and slotted ALOHA. A discussion of the timing of data generation in the SN, which is critical to the analysis of the AoI, was given in Section 2.2.

In the following chapters, we consider the AoI for the grant access scenarios and grant-free access scenario, respectively. In the next chapter, the AoI minimization problem for grant access schemes, TDMA and FDMA, will be first discussed.

# Chapter 3

# AoI Minimization Problems over Grant Access Schemes

In this chapter, we consider the grant access schemes such as TDMA and FDMA, and proposes a novel resource allocation algorithm for minimizing AoI in these schemes.

We first explain the definition of AoI in the simplest scenario where a single SN communicates with a FC. After that, the description is extended to a multiple SNs environment, the optimization problem for minimizing AoI in TDMA and FDMA is defined, and a novel resource allocation algorithm is proposed.

## 3.1 Single SN-FC Link

For the sake of completeness and clarity of exposition, we first consider a simple scenario in which a single SN communicates with the FC, as studied in [33], and the indices are omitted in this section. Then, the capacity of the corresponding channel for a fixed $h$ can be written as

$$C \triangleq B \log_2 \left(1 + |h|^2 \frac{kE}{nBN_0}\right), \tag{3.1}$$

where $B$ is the bandwidth assigned to the SN.

We observe that the SN can successfully transfer its $D$-bit data to the FC if and only if the total information communicated at best at the rate $C$ over the transmission time $n$, exceeds $D$. In other words, the following condition must be satisfied in order for the delivery to be successful

$$D \leq nC. \tag{3.2}$$

Following related literature [20, 33], the AoI of the SN is the reward over the total elapsed time, including the harvesting time $k$ and the data transmission time $n$, *i.e.*

$$P \triangleq \frac{1}{2}(k+n)^2. \tag{3.3}$$

Given the above, we now consider the AoI minimization problem subject to the throughput requirement given in the inequality (3.2), namely

$$\underset{k,n}{\text{minimize}}\ P, \tag{3.4a}$$

$$\text{subject to } D \leq nC. \tag{3.4b}$$

Substituting (3.1) into (3.2) and expressing the harvesting time $k$ that satisfies the constraint of inequality (3.2), we obtain

$$k \geq \left\lceil \frac{nBN_0}{|h|^2 E} \left(2^{\frac{D}{nB}} - 1\right) \right\rceil, \tag{3.5}$$

such that the minimum harvesting time $k$ as a function of the transmission time $n$ can be obtained from the lower bound of the latter inequality, *i.e.*,

$$k(n) = \frac{nBN_0}{|h|^2 E} \left(2^{\frac{D}{nB}} - 1\right), \tag{3.6}$$

where $n$ and $k(n)$ are relaxed as positive real values $\mathbb{R}^+$.

By combining equations (3.3) and (3.6), the AoI can be expressed as a function of $n$, namely

$$f(n) = \frac{1}{2}(k(n)+n)^2. \tag{3.7}$$

Owing to the relaxation in equation (3.6), the function $f(n)$ in equation (3.7) can be considered as a lower bound of the AoI $P$, such that the constrained optimization problem in equation (3.4) is an equivalent unconstrained problem

$$\underset{n}{\text{minimize}}\ f(n). \tag{3.8}$$

Although $k$ and $n$ are treated as positive real numbers in the above, we shall hereafter limit these quantities to positive integer (*i.e.*, natural) values to accommodate for the discrete nature of packetized TDMA networks as well as of synchronous FDMA schemes. Since the solution of equation (3.8) is generally not integer, the desired solution of the problem will be taken as a projection of the solution $n^*$ of (3.8) onto the feasible set, namely, $(\lceil n^* \rceil, \lceil k(n^*) \rceil)$.

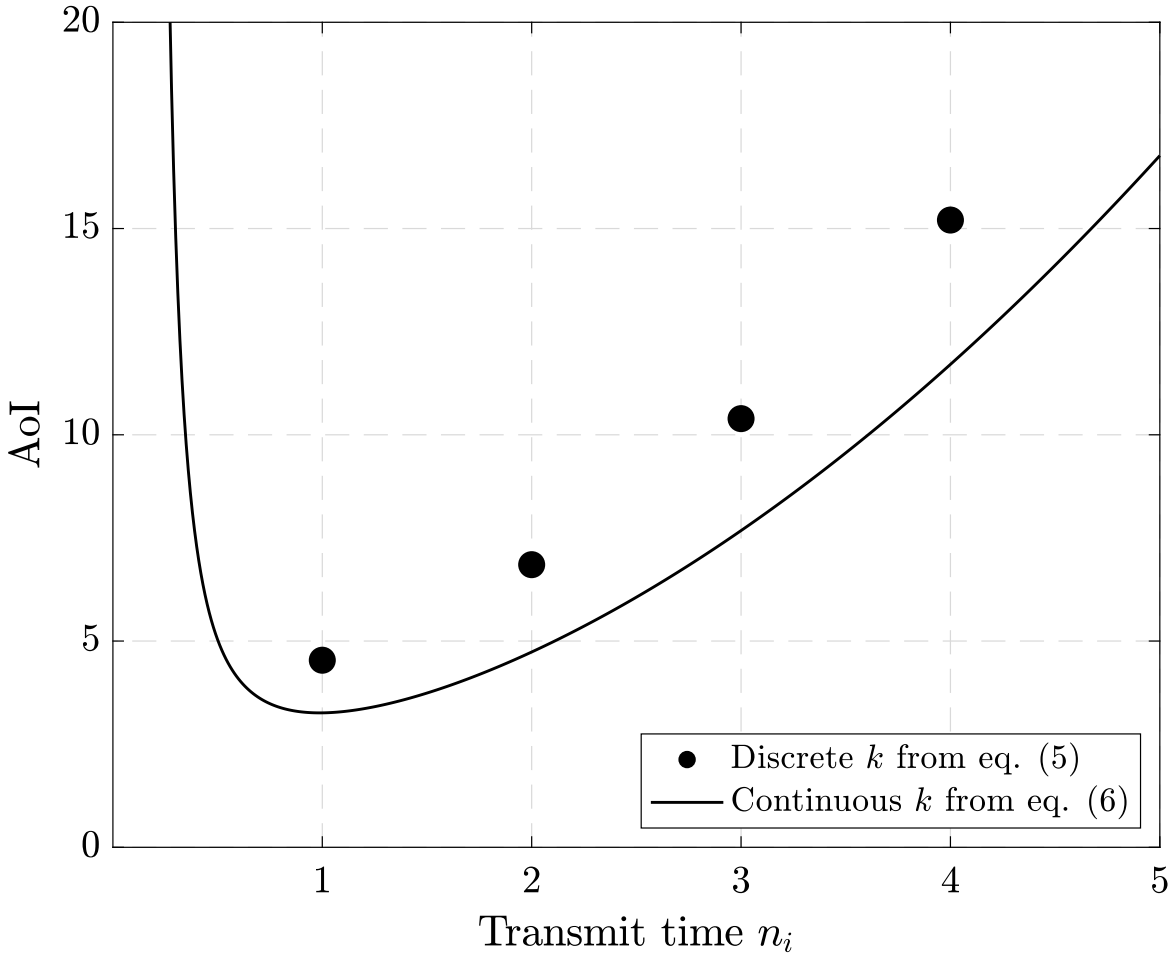


Fig. 3.1 Average AoI with continuous and discrete transmission and harvesting times, for a single-SN system with $D = 1$ [Mbit], $E = 1.0$ [mW], and base SNR $\triangleq \frac{\mathbb{E}[|h|^2]}{BN_0} = 30$ [dB].

A comparison between the average AoI achievable with continuous versus discrete times is shown in Fig. 3.1. To be more specific, the figure exhibits plots of $\mathbb{E}[f(n)]$ with $f(n)$ as in equation (3.7), respectively with $n \in \mathbb{R}^+$ and $k(n)$ as in equation (3.6) averaged over multiple realizations of $h$, and with the transmission and harvesting times projected to their closest upper-bounding integers $(\lceil n^* \rceil, \lceil k(n^*) \rceil)$. It can be seen that a fundamental penalty is paid for the discretization of time required by synchronous access schemes such as TDMA and FDMA, which increases with the transmission time $n$.

We emphasize also that such a penalty does not include the possible sub-optimality incurred by projecting the real-valued solution of the problem in equation (3.8) onto $\mathbb{N}$, as opposed to solving the problem directly over $\mathbb{N}$, which however is NP-hard.

To conclude this subsection, we address the solution of the AoI minimization problem given by equation (3.7), which is facilitated by the following two results.

**Proposition 1** *With $E > 0$, $D > 0$, $B > 0$, $N_0 > 0$, $|h|^2 > 0$, $\beta \triangleq BN_0/E$, and $\gamma \triangleq D/B$, the AoI $f(n)$ given by equation* (3.7) *is convex with respect to n.*

*Proof:* See Appendix A.

■

**Proposition 2** *For $\gamma > 0$ and $\beta > 0$, the unique solution $n^*$ of the minimization problem described by equation* (3.8) *can be obtained by solving the implicit equation*

$$\frac{\beta}{|h|^2}\left(2^{\frac{\gamma}{n}}-1\right)-\frac{\beta\gamma\log(2)}{|h|^2 n}2^{\frac{\gamma}{n}}+1=0. \tag{3.9}$$

*Proof:* See Appendix B.

■

Finally, we introduce the main result of this subsection, in the form of the following Proposition.

**Proposition 3** *For $\gamma > 0$ and $\beta > 0$, the solution of equation* (3.9)*, i.e., the transmission time $n^*$ that minimizes the AoI in the single SN-FC link, is bounded by*

$$n_L^* \triangleq \frac{\gamma}{\log_2\left(e-1+\frac{|h|^2}{\beta}\right)} \leq \underbrace{n^* \leq \gamma\log 2 \triangleq n_U^*}_{\forall\, |h|^2>\beta}, \tag{3.10}$$

*where we emphasize that the condition $|h|^2 > \beta$ is only required for the upper-bounding relation to hold.*

*Proof:* See Appendix C.

■

## 3.2 Multiple SN-FC Links

Taking advantage of the formulation presented above, we now consider a more general scenario where $N$ SNs simultaneously transmit, with the help of either a TDMA or an FDMA scheme, to a common FC, proposing two corresponding resource allocation schemes optimized to minimize the mean AoI of both systems.

To this end, we first define the mean conditional[1] AoI minimization problem associated with a scenario with $N$ SNs, which can be expressed as

$$\underset{\boldsymbol{n}}{\text{minimize}} \ \frac{1}{N}\sum_{i=1}^{N} f(n_i), \tag{3.11}$$

where $\boldsymbol{n} \triangleq \{n_1, n_2, \ldots, n_N\}$..

### 3.2.1 Time Division Multiple Access Systems

To avoid interference among the $N$ SNs, in a TDMA scheme the entire bandwidth available in the system $B_{\text{total}}$ is assigned to a single SN during its transmission time interval $n_i$. In other words, we have

$$B_i = B, \forall \, . \tag{3.12}$$

For the sake of simplicity, it shall also be assumed hereafter that all SNs are subjected to the same conditions, such that the average harvested energy $E$ and the amount of data to be transmitted $D$ are the same for all SNs.

Finally, under a TDMA scheme, only one SN is allowed to transmit during its allocated time, which can be expressed by the constraint

$$\sum_{i=1}^{N} \mathbb{1}_i(t) \leq 1, \tag{3.13}$$

where $\mathbb{1}_i(t)$ is an indicator function that takes the value 1 at $k_i < t \leq (k_i + n_i)$ and 0 elsewhere.

Taking into account the above constraints, the resource allocation problem to minimize the average AoI in TDMA can be formulated as

$$\underset{\boldsymbol{n}}{\text{minimize}} \ \frac{1}{N}\sum_{i=1}^{N} f(n_i), \tag{3.14a}$$

$$\text{subject to} \ \sum_{i=1}^{N} \mathbb{1}_i(t) \leq 1, \forall 0 \leq t \leq k_N + n_N. \tag{3.14b}$$

In order to gain insight on how to solve the problem described above in a general setting, we first consider a particular case with only two SNs, labeled $\text{SN}_1$ and $\text{SN}_2$. Following our notation, the optimal transmission times associated with these two SNs will be denoted $n_1^*$

[1] Here, the term mean refers to the average taken over the multiple SNs, while the term condition refers to the fact that the channel gains $h$ are assumed to be constant.

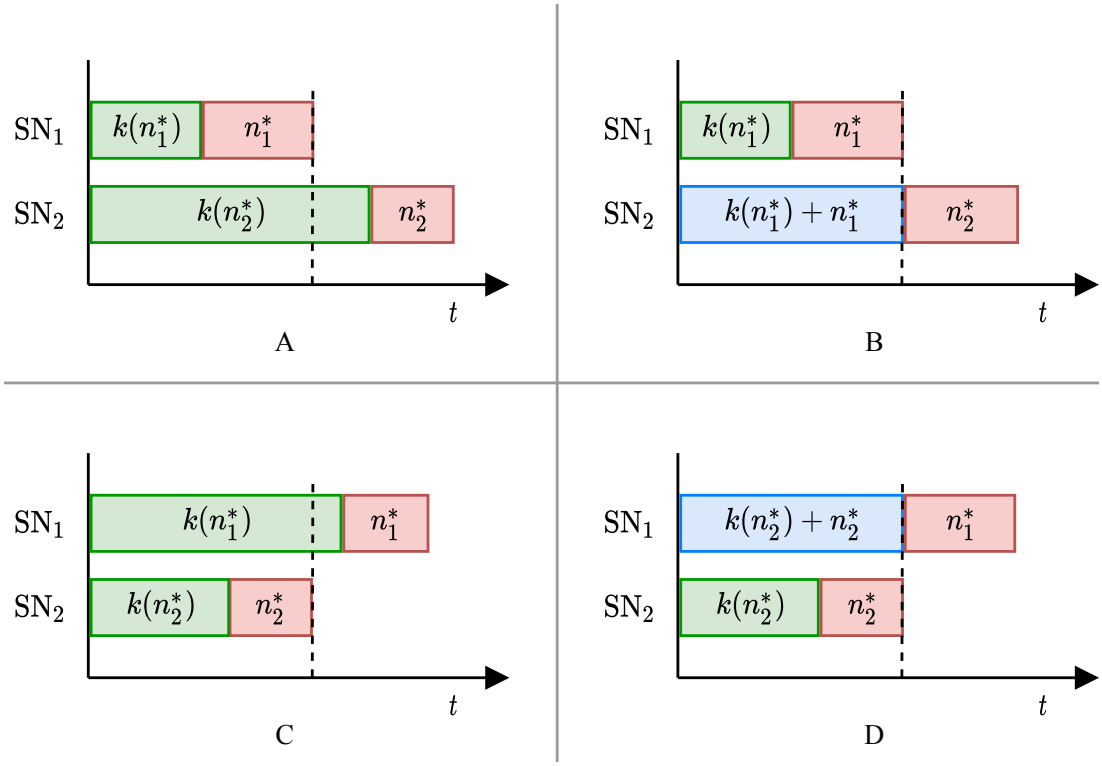


Fig. 3.2 Illustration of the four allocation arrangements in a TDMA-based EH-WSN with two SNs and one FC.

and $n_2^*$, respectively, with their corresponding minimum energy harvesting times, obtained from equation (3.6), denoted accordingly by $k(n_1^*)$ and $k(n_2^*)$.

Referring to Fig. 3.2, it is evident that in this case, the problem of minimizing the mean conditional AoI reduces to determining which of the two nodes shall transmit first, a decision which is informed by whether the time taken by the first node to complete its harvesting-and-transmission cycle is sufficient to enable the second node to harvest enough energy for its own transmission.

In other words, the optimal time allocation is fundamentally driven by the tests $k(n_2^*) \gtrless k(n_1^*) + n_1^*$ and $k(n_1^*) \gtrless k(n_2^*) + n_2^*$, with the best strategy being given by the one in which the SN second to transmit has enough time to harvest all the required energy during the transmission of the first node, such that its transmission can start immediately after the first.

To elaborate further, following the illustration in Fig. 3.2, there are four distinct cases to be considered, namely:

$$\bar{f}_A(n_1^*,n_2^*) = \frac{1}{2}\left(k(n_1^*)+n_1^*\right)^2 + \frac{1}{2}\left(k(n_2^*)+n_2^*\right)^2, \tag{3.15a}$$

$$\bar{f}_B(n_1^*,n_2^*) = \frac{1}{2}\left(k(n_1^*)+n_1^*\right)^2 + \frac{1}{2}\left(k(n_1^*)+n_1^*+n_2^*\right)^2, \tag{3.15b}$$

$$\bar{f}_C(n_1^*,n_2^*) = \frac{1}{2}\left(k(n_2^*)+n_2^*\right)^2 + \frac{1}{2}\left(k(n_1^*)+n_1^*\right)^2, \tag{3.15c}$$

$$\bar{f}_D(n_1^*,n_2^*) = \frac{1}{2}\left(k(n_2^*)+n_2^*\right)^2 + \frac{1}{2}\left(k(n_2^*)+n_2^*+n_1^*\right)^2, \tag{3.15d}$$

where $\bar{f}(n_1,n_2) \triangleq \frac{f(n_1)+f(n_2)}{2}$ and the indices $A,B,C$ and $D$ represent the four distinct possibilities as illustrated.

It can be seen that the cases $A$ and $C$, with corresponding mean conditional AoI given by (3.15a) and (3.15c), respectively, are inefficient because they cause the channel to remain idle after the first to transmit SN completes its cycle, while SN second to transmit harvests the required energy for its own transmission. It follows therefore that the optimum allocation strategy in this particular setting of two SN lays in between the cases $B$ and $D$. Furthermore, it is evident that the optimum choice between these two options is governed by the test

$$\bar{f}_B \underset{\mathrm{SN}_1\to\mathrm{SN}_2}{\overset{\mathrm{SN}_2\to\mathrm{SN}_1}{\gtrless}} \bar{f}_D, \tag{3.16}$$

which, if stated in words, signifies that the transmission order $\mathrm{SN}_2$ followed by $\mathrm{SN}_1$ is optimal if $\bar{f}_B > \bar{f}_D$, whereas the order $\mathrm{SN}_1$ followed by $\mathrm{SN}_2$ is optimal if $\bar{f}_B < \bar{f}_D$.

In light of the above, we consider the following results.

**Proposition 4** *For $\gamma > 0$ and $\beta > 0$,*

$$|h_1|^2 > |h_2|^2 \implies n_{1L}^* < n_{2L}^*, \tag{3.17a}$$

$$n_{1U}^* = n_{2U}^*. \tag{3.17b}$$

*Proof:* See Appendix D.

■

**Proposition 5** *For $\gamma > 0$ and $\beta > 0$,*

$$|h_1|^2 > |h_2|^2 \implies k(n_{1L}^*;h_1) < k(n_{2L}^*;h_2), \tag{3.18a}$$

$$|h_1|^2 > |h_2|^2 > \beta \implies k(n_{1U}^*;h_1) < k(n_{2U}^*;h_2), \tag{3.18b}$$

**Algorithm 1** Greedily-initialized TDMA AoI minimizer

**Inputs:** $E > 0$, $D > 0$, $B > 0$, $N_0 > 0$ and $|h_i|^2 > 0$, with $i \in \boldsymbol{N} \triangleq \{1,\dots,N\}$.
**Outputs:** Optimal transmission time $\boldsymbol{n}^* \in \mathbb{R}^+$ and optimal harvested time $\boldsymbol{k}^* \in \mathbb{R}^+$.

**Initialization:**
Set loop counter $i = 1$.
Set initial transmission times $\boldsymbol{n} \gg 1$.
Set initial harvesting times $\boldsymbol{k} = 0$.
Sort SN indices $\boldsymbol{N}$ such that $|h_1|^2 > \cdots > |h_N|^2$.
**Core Procedure:**
**while** $|\boldsymbol{N}| \geq 2$ **do**
    Find the optimal $n_i^*$ and $n_{i+1}^*$ by solving (A.1c).
    **if** $\bar{f}_B(n_i^*, n_{i+1}^*) > \bar{f}_D(n_i^*, n_{i+1}^*)$ **then**
        Swap indices $i$ and $i+1$
    **end if**
    **if** $i \geq 2$ and (3.14b) is not satisfied **then**
        Update $k(n_i) = k(n_{i-1}) + n_{i-1}$
    **end if**
    Update $\boldsymbol{N} \leftarrow \boldsymbol{N} \setminus i$
    Append $\boldsymbol{n}^*$ with $n_i$ and $\boldsymbol{k}^*$ with $k(n_i)$
    Update $i \leftarrow i+1$.
**end while**

*where the bounding quantities* $(n_{1L}^*, n_{1U}^*)$ *are as defined in Proposition 3 and its proof.*

*Proof:* See Appendix E. ■

**Proposition 6** *For* $\gamma > 0$ *and* $\beta > 0$*,*

$$\bar{f}_B(n_{1L}^*, n_{2L}^*) < \bar{f}_D(n_{1L}^*, n_{2L}^*), \tag{3.19a}$$

$$\bar{f}_B(n_{1U}^*, n_{2U}^*) < \bar{f}_D(n_{1U}^*, n_{2U}^*). \tag{3.19b}$$

*Proof:* See Appendix F. ■

We remark that setting $|h_1|^2 > |h_2|^2$ is without loss of generality as it amounts merely to ordering the SNs. Although a closed-form expression of the optimum transmission times $n_1^*$ and $n_2^*$ cannot be obtained, Proposition 6 in fact establishes that, given knowledge of $|h_1|^2$ and $|h_2|^2$ only, the wisest TDMA allocation strategy in a system with two SNs is a "*greedy*"

scheme in which the SN with the strongest channel gain precedes the other SN, since under such a strategy both the lower and upper bounds on the mean AoI $\bar{f}_B(n_1^*, n_2^*)$ are inferior to those of the alternative "*Robin Hood*" (the weaker SN first) strategy of allocating times the other way around.

Furthermore, the impossibility to be certain of the optimality of the greedy allocation does *not* detract from the overall optimality of the TDMA strategy described, because the optimality of the initial choice can be easily verified (and if necessary reverted) by solving equation (3.9) via a simple bisection algorithm, which is only made more efficient given the assured bounds offered in Propositions 4 and 5.

Next, we consider a more general setting, where $N$ SNs communicate with the FC through a TDMA scheme. In this case, referring to Fig. 3.2, it is evident that since all SNs stay in EH mode while the greedily-selected SNs transmit, after a sufficiently large number of SNs have transmitted the order of the remaining SNs is irrelevant to optimality.

In other words, the uncertainty of the channel power-based greedy selection between any pair of SNs $(i, i+1)$ decreases with $i$. Taking all the above into consideration, an optimal TDMA strategy to minimize the average AoI can be obtained for the general system with $N$ SNs, by repeating the pair-wise greedy-selection described above.

In summary, the optimal TDMA strategy is therefore:

1. Sort the indices SNs in descending order of channel power, such that $|h_1|^2 > \cdots > |h_N|^2$;
2. Set $i = 1$ and solve equation (3.9) via bisection using the bounds in inequalities (3.17) only for two strongest SNs, obtaining $n_i^*$ and $n_{i+1}^*$;
3. If and only if all remaining nodes have not harvested enough energy, and
4. Allocate $n_i^*$, and remove $i$ index from the list $\boldsymbol{N}$;
5. Repeat steps 2 to 4 until there is only one SN left, which is allocated last.

The pseudocode corresponding to the TDMA allocation procedure described above that minimizes the mean AoI of an EH-WSNs with $N$-SNs is shown in Algorithm 1.

### 3.2.2 Frequency Division Multiple Access Systems

In contrast to the TDMA scheme, in an FDMA system, SNs can transmit data to the FC and in an orthogonal manner, at the expense of a reduction in the bandwidth $B_i$ used by each

SN, which is a fraction of the total available bandwidth $B_{\text{total}}$. In this case, the mean AoI minimization problem can be written as

$$\underset{\boldsymbol{n},\,\boldsymbol{B}}{\text{minimize}}\ \frac{1}{N}\sum_{i=1}^{N} f(n_i, B_i), \tag{3.20a}$$

$$\text{subject to } B_{\text{total}} - \sum_{i=1}^{N} B_i = 0, \tag{3.20b}$$

where $\boldsymbol{B} \triangleq \{B_1, B_2, \ldots, B_N\}$.

Since the objective function given (3.20a) involves a coupled expression of the optimization variables $\boldsymbol{n}$ and $\boldsymbol{B}$, as shown in (3.6) and (3.7), it is difficult to solve the above optimization analytically and globally. Therefore, we resort to an alternating optimization framework where (3.20) is divided into optimization problems (I) and (II) as follows.
(I) Optimization problem for bandwidth allocation $\boldsymbol{B}$

$$\underset{\boldsymbol{B}}{\text{minimize}}\ \frac{1}{N}\sum_{i=1}^{N} f(B_i|n_i), \tag{3.21a}$$

$$\text{subject to } B_{\text{total}} - \sum_{i=1}^{N} B_i = 0. \tag{3.21b}$$

(II) Optimization problem for transmission time allocation $\boldsymbol{n}$

$$\underset{\boldsymbol{n}}{\text{minimize}}\ \frac{1}{N}\sum_{i=1}^{N} f(n_i|B_i). \tag{3.22}$$

Next, consider the following result.

**Proposition 7** *For $E_i > 0$, $|h_i|^2 > 0$, $N_0 > 0$, $D_i > 0$ and $n_i > 0$, the function $f(B_i|n_i)$ is convex with respect to $B_i$.*

*Proof:* Please see Appendix G .

■

The convexity of $f(B_i|n_i)$ established by Proposition 7 implies that problem (3.21) can be efficiently solved via the alternating direction method of multipliers (ADMM) [44].

**Algorithm 2** ADMM - BM AoI minimizer

**Inputs:** $E_i > 0$, $|h_i|^2 > 0$, $N_0 > 0$, $B_{\text{total}} > 0$, $B_i > 0$, $D_i > 0$, $n_i > 0$, $i \in \boldsymbol{N} \triangleq \{1,\ldots,N\}$, convergence range $\varepsilon$, and number of iterations for outer and inner loops $s_{\text{out}}^{\max}$ and $s_{\text{in}}^{\max}$.
**Outputs:** Optimal transmission times $\boldsymbol{n}^* \in \mathbb{R}^+$ and optimal bandwidths $\boldsymbol{B}^* \in \mathbb{R}^+$.

Initialize outer loop counter to $s_{\text{out}} = 1$.
Set initial transmission time $\boldsymbol{n}^{s_{\text{out}}} \gg 1$ and $\theta \gg 1$.
**while** $s_{\text{out}} \leq s_{\text{out}}^{\max}$ and $|\boldsymbol{n}^{s_{\text{out}}} - \boldsymbol{n}^{s_{\text{out}}-1}| > \varepsilon$ **do**
    Initialize the inner loop counter to $s_{\text{in}} = 1$.
    **while** $s_{\text{in}} \leq s_{\text{in}}^{\max}$ and $\theta > \varepsilon$. **do**
        Update $B_i^{s_{\text{in}}}$, $\theta^{s_{\text{in}}}$ and $u^{s_{\text{in}}}$ via equation (3.23).
        Update $s_{\text{in}} \leftarrow s_{\text{in}} + 1$.
    **end while**
    Find the $\boldsymbol{n}^{s_{\text{out}}}$ by solving (3.9).
    Update $s_{\text{out}} \leftarrow s_{\text{out}} + 1$.
**end while**
$\boldsymbol{n}^* = \boldsymbol{n}^{s_{\text{out}}}$ and $\boldsymbol{B}^* = \boldsymbol{B}^{s_{\text{in}}}$.

More specifically, following [44, 45], convex problems of the form described in (3.21) can be solved by successive iterations of the following steps:

$$\boldsymbol{B} \leftarrow \underset{\boldsymbol{B}}{\operatorname{argmin}}\, L_\rho(\boldsymbol{B}, B_{\text{total}}, u), \tag{3.23a}$$

$$\theta \leftarrow \Big(B_{\text{total}} - \sum_{i=1}^{N} B_i\Big), \tag{3.23b}$$

$$u \leftarrow u + \theta, \tag{3.23c}$$

where $\theta \in \mathbb{R}$ is an auxiliary variable, $u$ is the scaled dual variable, and $L_\rho(\boldsymbol{B}, B_{\text{total}}, u)$ is the associated augmented Lagrangian of the problem, which, for a penalty parameter $\rho > 0$, is given by

$$L_\rho(\boldsymbol{B}, B_{\text{total}}, u) = \sum_{i=1}^{N} f(B_i|n_i) + \frac{\rho}{2}\Big(B_{\text{total}} - \sum_{i=1}^{N} B_i + u\Big)^2 + \frac{\rho}{2}u^2. \tag{3.24}$$

Similarly, the convexity of $f(n_i|B_i)$ with respect to $n_i$ established by Proposition 1, together with the bounds on its minimizer established by Proposition 3, enables the efficient solution of problem (3.22) via the bisection method (BM). Altogether, using these two techniques, the optimum bandwidth and transmit time allocation problem (3.20) can be

obtained by solving equations (3.21) and (3.22) alternately. A pseudocode summarizing the method described above is given in Algorithm 2.

## 3.3 Chapter Summary

In this chapter, for grant access schemes, we first introduced the simple scenario where a single SN communicates with the FC and described the definition of the AoI and some important propositions. In section 3.2, after describing the inherent constraints and the AoI minimization problem in the two different multiaccess schemes, TDMA and FDMA, a novel resource allocation algorithm for each scheme is proposed.

# Chapter 4

# AoI over Grant-Free Access

In this chapter, we consider the EH-WSN with slotted ALOHA that is one of the grant-free access schemes, and investigate the average AoI. We first define the time slot and describe the protocol of our system, then provide the assumption for calculating the AoI in slotted ALOHA.

## 4.1 Slotted ALOHA with EH

In slotted ALOHA, time slots are used as a unit of time division, and each time slot consists of $T$ complex symbols when communicating with the total bandwidth $B_{\text{total}}$. Fig. 4.1 shows an illustration of the time axis comparison between slotted ALOHA and TDMA with the same bandwidth, from this figure, if the transmission need the transmission time $n_1$, transmission time slots is represented as $\lceil n_1/T \rceil = 3$ for $\text{SN}_1$ in sloted ALOHA. In contrast to TDMA where the FC determines the timing of transmission as shown in Fig. 4.1 (b), in slotted ALOHA, the timing of transmission depends on each SN, but if multiple SNs transmit in the same time slot data collision occur and the transmission fail (*e.g.*, Fig. 4.1 (a) in $j+1$th timeslot).

Next, we describe the protocol of slotted ALOHA with EH. Each SN selects the four states defined in the following during the transmission:

1. Sleep mode, where SNs do not have enough energy and they can harvest power from environmental sources.

2. Decision, where SNs have enough energy to transmit and they decide whether or not to transmit the data according to the transmission probability $p$.

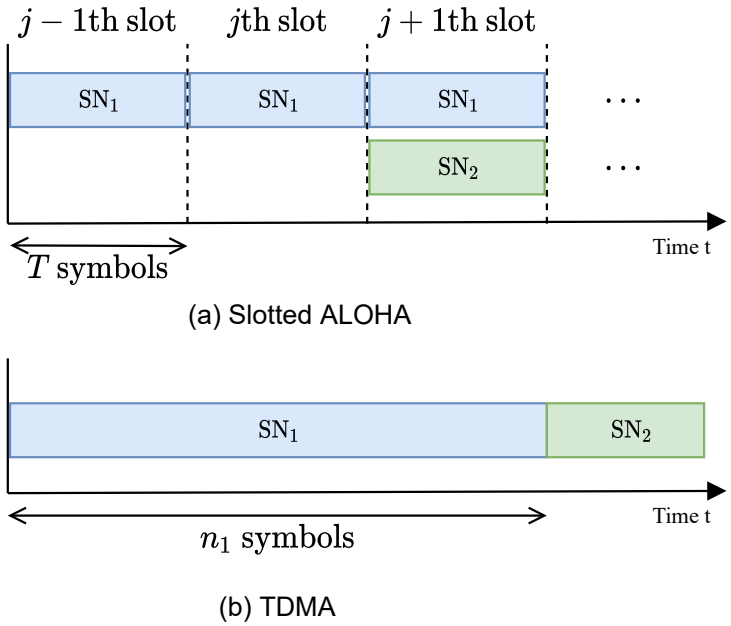


Fig. 4.1 Illustration of the time axis comparison between slotted ALOHA and TDMA

3. Transmission, where the SNs that decide to transmit data in active mode change to this state. If only one SN transmits the data, the FC can receive the data and sends the feedback beacon to the SN in order to indicate that the transmission is complete. Note that we assume that the feedback beacon can be sent back to the SN within the same transmission time slot and that the SN can receive this beacon correctly. If two or more SNs transmit data simultaneously, the data collide and the data transmission fails. If a data collision occurs and the FC does not receive anything, no feedback beacon is sent back to the SNs, so the SNs acknowledge the failure of their own data transmission and changes to sleep mode.

4. Completion, where SNs that received the beacon from FC move this state and wait until the other SN has completed transmission.

Finally, we explain in detail the flow from the time the system is started until all SNs transition to the "Completion" state. All SNs generate the information at the beginning of the system $t = 0$ (concurrent model) and then go to sleep mode. After the harvested enough energy to transmit, the state of SN transitions to the decision. The SN decided whether or not to transmit the data according to the transmission probability $p$. As the results of the above, if the SN does not transmit, it will remain decision state and wait for the next time slot. If only one SN is transmitting, the data transmission is complete, *i.e.*, if two or more SNs are in the middle of a transmission, a data collision will occur and the SNs will be in sleep mode. If

the data is transmitted without collision, the FC sends a feedback beacon to the SN that did the transmission. Finally, the SN that receives the beacon move to the completion state, and these processes continue until all SNs have completed their data transmission. A flowchart illustrating the above process is shown in Fig. 4.2.

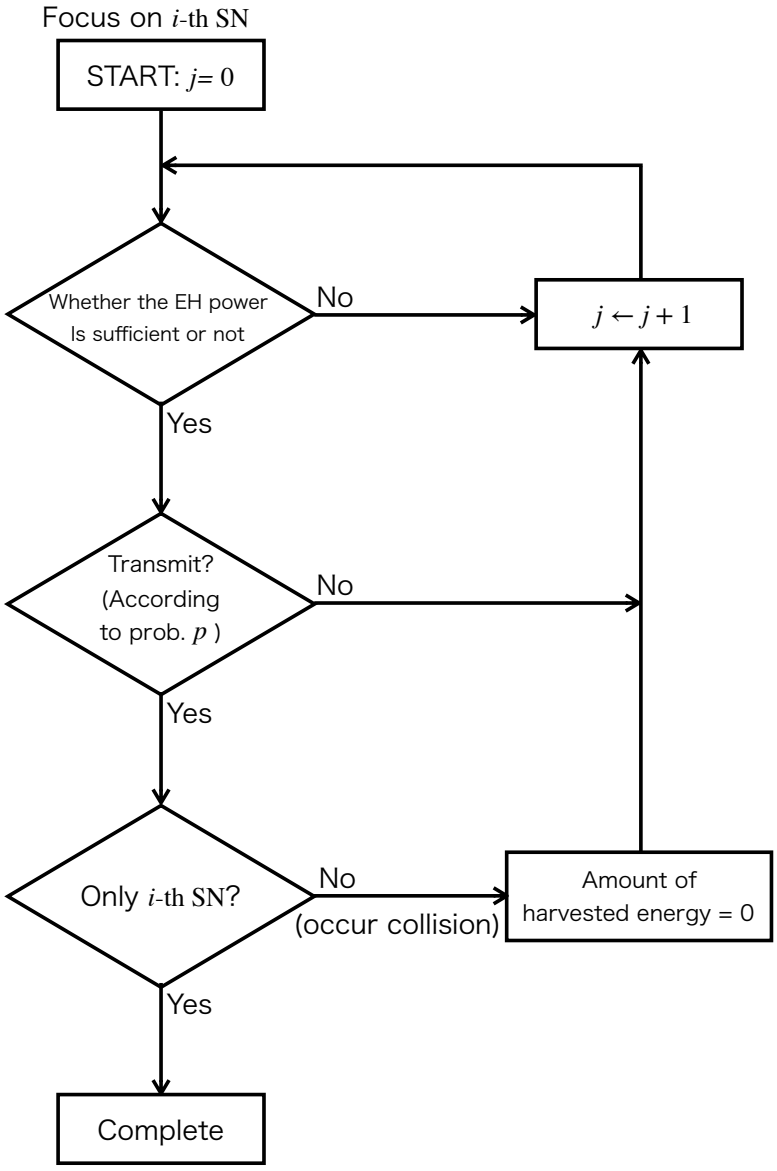


Fig. 4.2 Flowchart for slotted ALOHA: The $i$-th SN focus on proceeds in the direction of the arrow, through a number of questions (in the frame represented by the diamond), until it finally reaches "complete". Variable $j$ is the time-slot index.

## 4.2 AoI Expression in Slotted ALOHA

In this chapter, we describe the average AoI per SN in slotted ALOHA. First of all, we define $m$ as the time slot, which is the smallest unit of time in the slotted ALOHA and we assume that $m = T$ given some $T$.

Fig. 4.3. shows an illustration of transmission in a slotted ALOHA with EH. Using the time slot $m$, the harvested time $k_{\mathrm{SA},i}$ and the transmission time $n_{\mathrm{SA},i}$ in the slotted ALOHA can be expressed as follows,

$$k_{\mathrm{SA},i} = \left\lceil \frac{k_i}{m} \right\rceil, \tag{4.1}$$

$$n_{\mathrm{SA},i} = \left\lceil \frac{n_i}{m} \right\rceil. \tag{4.2}$$

As in TDMA, each SN communicates with the FC over the entire system bandwidth $B_{\mathrm{total}}$, and the channel capacity $C_{\mathrm{SA}}$ and the condition that each SN must satisfy are expressed using the transmission time slots $n_{\mathrm{SA},i}$ as follows,

$$C_{\mathrm{SA},i} \triangleq B_{\mathrm{total}} \log_2 \left( 1 + |h_i|^2 \frac{k_i E}{n_{\mathrm{SA},i} B_{\mathrm{total}} N_0} \right), \tag{4.3}$$

$$D \leq n_{\mathrm{SA},i} \times C_{\mathrm{SA}}, \tag{4.4}$$

Substituting (4.3) in (4.4), the harvesting time $k_i$ is given by

$$k_i \geq \frac{n_{\mathrm{SA},i} B_{\mathrm{total}} N_0}{|h_i|^2 E} \left( 2^{\frac{D}{n_{\mathrm{SA},i} B_{\mathrm{total}}}} - 1 \right), \tag{4.5}$$

From equations (4.1) and (4.5), the harvested time for the slotted ALOHA can be expressed again as follows,

$$k_{\mathrm{SA},i} = \left\lceil \frac{n_{\mathrm{SA},i} B_{\mathrm{total}} N_0}{m |h_i|^2 E} \left( 2^{\frac{D}{n_{\mathrm{SA},i} B_{\mathrm{total}}}} - 1 \right) \right\rceil. \tag{4.6}$$

As the result of the above, the average AoI per SN to be calculate in numerical results is then defined as follows,

$$\frac{1}{2N} \sum_{i=1}^{N} (k_{\mathrm{SA},i} + n_{\mathrm{SA},i} + T_{w,i})^2, \tag{4.7}$$

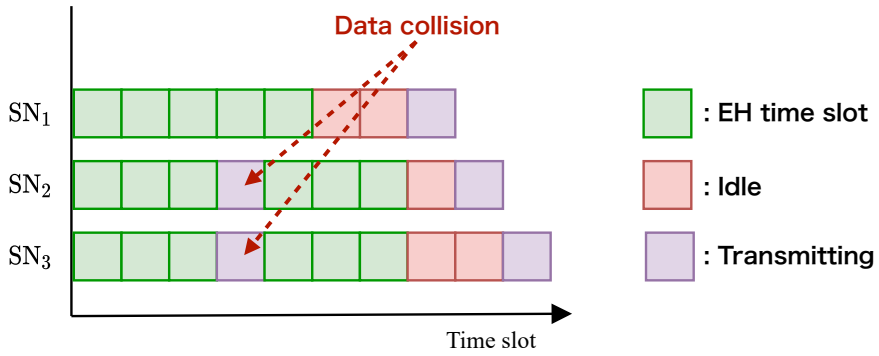


Fig. 4.3 Illustration of transmission in slotted ALOHA with three EH-SNs. One square represents a unit time slot $m$. We assume that the transmission time slot $n_{\mathrm{SA},i}(i \in 1,2,3) = m$ and each harvested times $k_{\mathrm{SA},1} = 5$, $k_{\mathrm{SA},2} = 3$, and $k_{\mathrm{SA},3} = 3$ are required respectively. In the 4th time slot, a data collision occurs and $\mathrm{SN}_2$ and $\mathrm{SN}_3$ need to re-harvest energy.

where $T_{w,i}$ is the total number of time slots, such as the waiting time for transmission and EH time after transmission failure, excluding first EH time $k_{\mathrm{SA},i}$ and transmission time $n_{\mathrm{SA},i}$.

## 4.3 Chapter Summary

In this chapter, we formulate the AoI differently from Chapter 3 for slotted ALOHA, which is one of the grant-free access. After we categorized the state of the SN in each time slot, we described the state transitions of the SN from the beginning of the system to the completion of data transmission.

In the next chapter, we present numerical results illustrating the performance of the AoI for each of the multiple access methods described in Chapter 3 and this chapter.

# Chapter 5

# Numerical Results

In this section, we present numerical results build on the analysis and algorithms and reveal the impact of both EH and multiple access strategies on the achievable AoI of WSNs. To this end, we first evaluate the performance of the proposed optimization algorithms in terms of the average AoI values in TDMA and FDMA scenarios and over fading channels. After that, we investigate the AoI performance of the slotted ALOHA and compared this scheme to TDMA with an overhead as a benchmark.

## 5.1 AoI Evaluations of Grant Access Schemes

Following a related study [17, 46], we set the total bandwidth and noise power spectrum density of the system to $B_{\text{total}} = 1$ [MHz] and $N_0 = 10^{-17}$ [mW/Hz], respectively, and assume that $h_i$ follows independent and identically distributed (i.i.d.) Gaussian distributions (Rayleigh fading channel) with the SNs and the FC separated by a distance of 1 [km] and the path loss for that distance set to 100 [dB]. Finally, the volume of information transmitted is set to $D_i = 1$ [Mbit], and the average EH rate (*i.e.*, the expected EH power) is set to $E_i = 1.0$ [mW] for all SNs.

Fig. 5.1 shows the average AoI performance, as a function of the number of SNs in the system, achieved by Algorithms 1 and 2 in such a scenario with TDMA and FDMA. More specifically, Fig. 5.1a shows results for the concurrent case of *e.g.* in [30, 33], when the sensed information is obtained simultaneously by all SNs and them transmitted after the SNs the required energy is harvested.

The figure shows also results obtained without the EH constraint, which can be taken as a lower bound on the average AoI, since no additional time is required to wait for the SNs to energize before transmitting.

It can be seen that in this case FDMA outperforms TDMA, although only mildly so in systems of small size. This is because, in TDMA schemes, the SNs must wait not only for their own EH cycles but also for preceding SNs complete their transmissions, before they themselves can transmit.

It is also found, however, that FDMA schemes exhibit a wider gap between the AoIs achieved with and without EH constraints, which increases as the size of the system grows. In contrast, the "EH penalty" paid by the TDMA scheme is significantly smaller and less dependent on the size of the system. To understand this result, recall that indeed in a TDMA system, the time consumed by EH cycles is only of relevance in the allocation of the first SNs to transmit, since all other SNs allocated later slots will, with great likelihood, have already harvested enough energy to carry out their transmissions by the time their allocated slots come due.

Next, Fig. 5.1(b) compares the average AoI obtained under a distributed sampling model such as that assumed *e.g.* in [29], showing results entirely opposite to those of Fig. 5.1(a). In this case, it is found that TDMA is superior to FDMA, with the difference between these two access schemes becoming increasingly significant as the number of SNs grows. Indeed, we note that an FDMA scheme in a strict sense – namely, in which SNs are allocated their own dedicated bands within which to transmit – is too "static" to comport the required dynamics of varying EH and sampling times faced in a WSN operating under a distributed sampling paradigm. It is this feature that makes the FDMA approach less flexible[1], as observed both in Figs. 5.1(a) and 5.1(b).

The findings observed above are confirmed and made more evident in the results shown in Fig. 5.2, in which the average AoI of the optimized TDMA and FDMA schemes, both under concurrent and distributed sampling and as functions of the EH power, are compared for systems with $N = 4$ and $N = 7$ SNs, with the remaining parameters identical to those of Fig. 5.1. It is found that under the distributed sampling model TDMA maintains, compared to FDMA, a lower AoI value regardless of the amount of EH power available or the number of SNs in the system, with the gap only growing with $N$, as already verified also in Fig. 5.1.

Under a concurrent sampling model, however, it is again found that FDMA can outperform TDMA, as long as the EH power available and/or the number of SNs in the system are/is sufficiently large. All in all, the results of Fig. 5.2 points for a localized optimality of FDMA, that is, under certain conditions, but an overall greater robustness TDMA schemes, with respect to the sampling model, system size, and available EH power.

[1] One can argue that an FDMA scheme with dynamically allocated bands would resolve this limitation. That would, however, require that the FC is aware of the instantaneous data volumes $D_i$ of all SNs, which would be impractical.

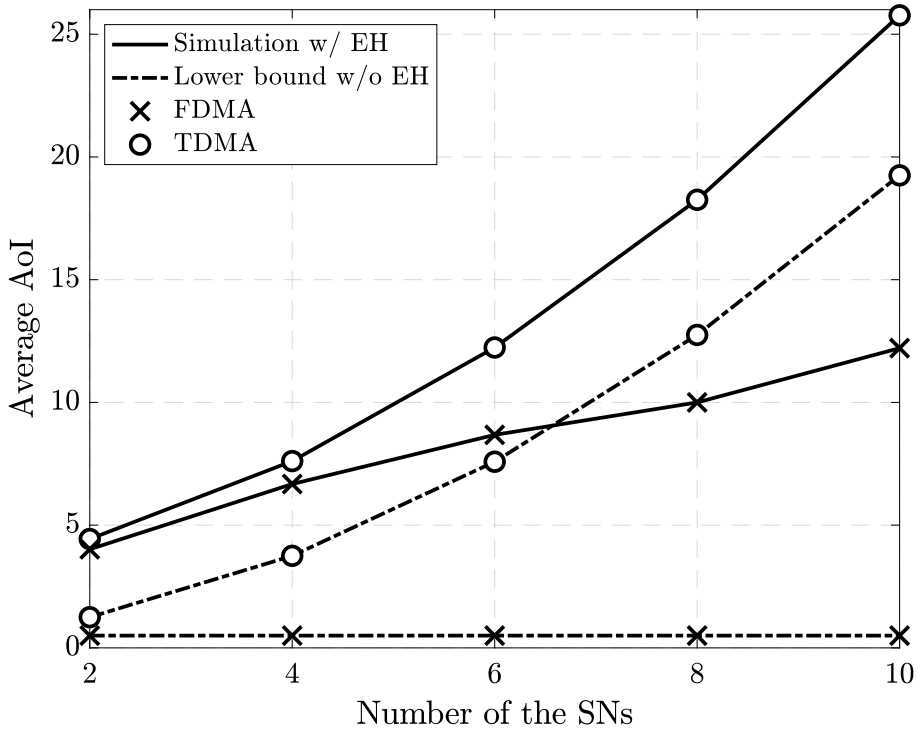


(a) Concurrent sampling model *e.g.* [30, 33].

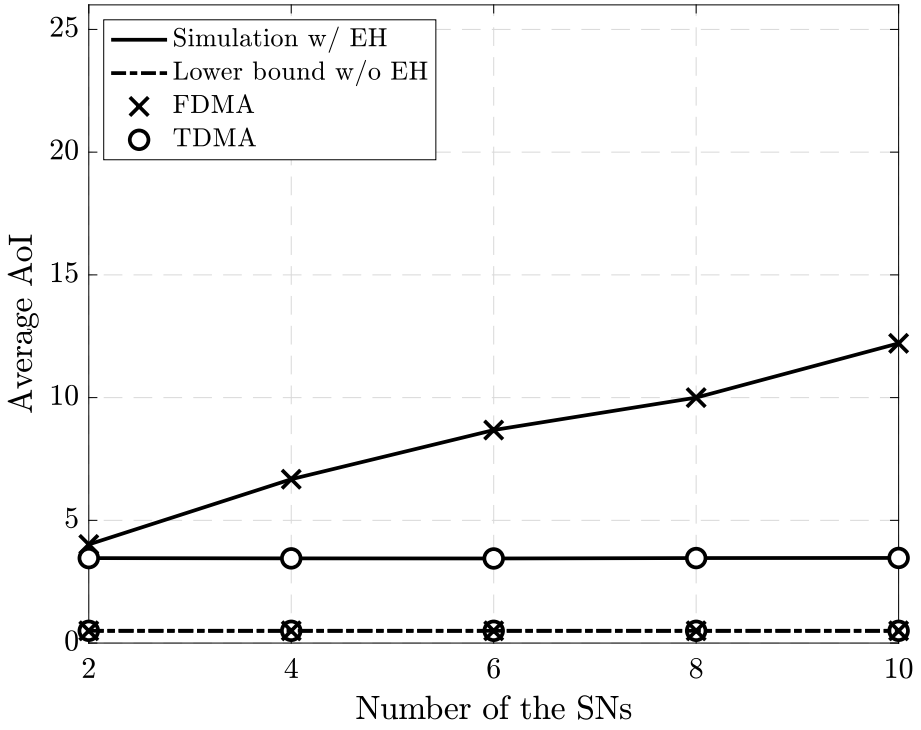


(b) Distributed sampling model *e.g.* [29].

Fig. 5.1 Average AoI as a function of the number of SNs in TDMA and FDMA with i.i.d. Rayleigh channels.

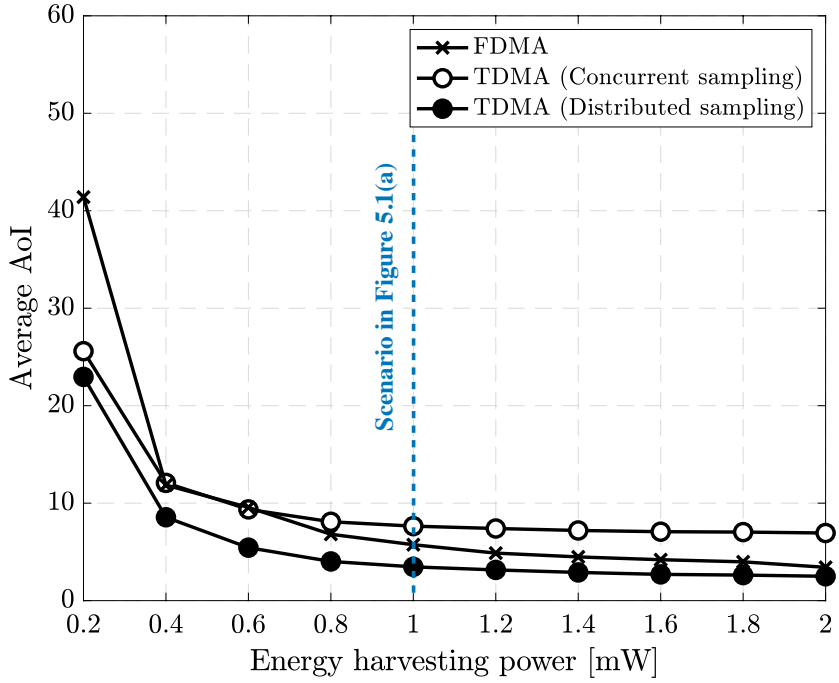


(a) Number of SNs: $N = 4$.

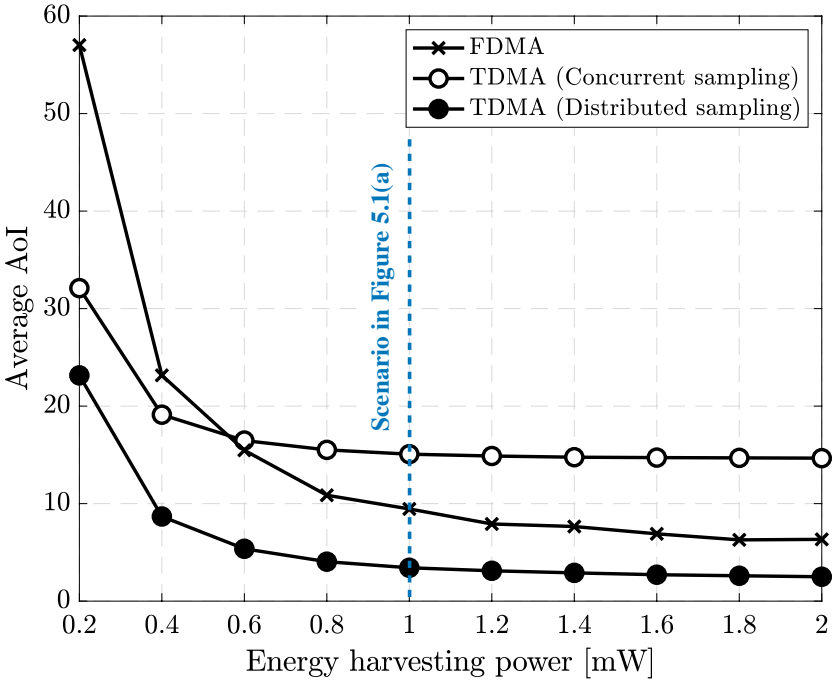


(b) Number of SNs: $N = 7$.

Fig. 5.2 Average AoI as a function of EH power in TDMA and FDMA systems.

This conclusion is only made clearer by the results of Fig. 5.3, where the average AoI achieved by the optimized TDMA- and FDMA-based EH wireless sensor networks, plotted as functions of the size of data packets, with $E_i = 1.0\,[\mathrm{mW}]$, both under concurrent and distributed sampling are compared, for systems with $N = 4$ and $N = 7$ SNs, with the remaining parameters identical to those of Fig. 5.1. Noticing that an increase of the data volume $D_i$, with the EH power kept fixed, amounts to making the EH constraint more stringent, it is non-surprising that it is found that under such conditions the FDMA approach proves increasingly inadequate as the $D_i$ grows.

It can therefore be reasonably concluded, with all relevant parameters taken into account jointly, that TDMA is a more robust multi-access scheme than FDMA for EH-WSNs, with the remark that punctually, depending on specific conditions, the FDMA might be a better choice.

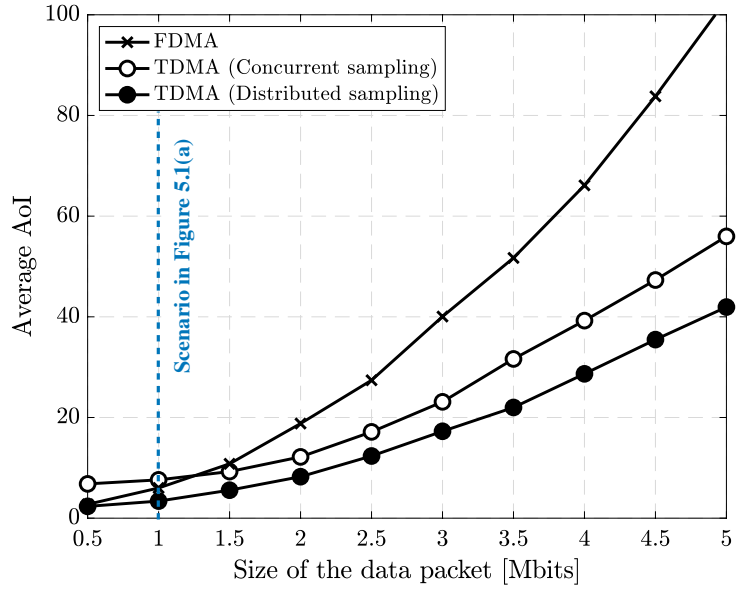


(a) Number of SNs: $N = 4$.

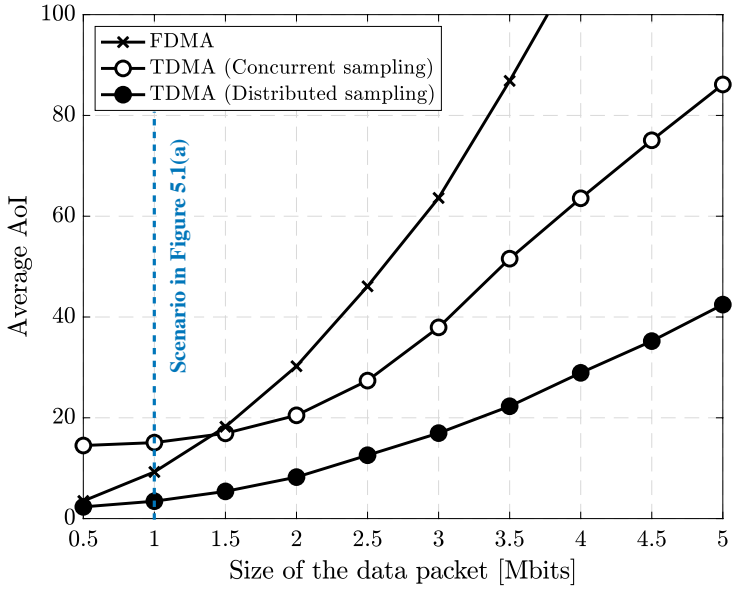


(b) Number of SNs: $N = 7$.

Fig. 5.3 Average AoI as a function of the size of data packets in TDMA and FDMA systems.

## 5.2 AoI Evaluations of Grant-Free Access

First, we describe a method for calculating the AoI of TDMA that considers the overhead to be compared with slotted ALOHA. Fig. 5.4 shows the example of time allocation in TDMA that considers the overhead, as can be seen from the figure, immediately after the system starts $t = 0$, all SNs are waiting to receive the allocation scheduling information from the FC, and this waiting time is determined by the ratio of the allocation information $D_O$ and the amount of transmission data $D$, which is defined as the overhead $T_O$, *i.e.*,

$$T_O \triangleq \frac{D_O}{D}. \tag{5.1}$$

Each SN then harvests the energy required for the optimal transmission time, as described in Chapter 3.2.1, and the harvested time is defined as follows

$$k(n_i) = \begin{cases} k(n_i^*) & (k(n_i^*) > k(n_{i-1}^*) + n_{i-1}) \quad (5.2) \\ k(n_{i-1}^*) + n_{i-1} & (otherwise) \quad (5.3) \end{cases}$$

From the above, the average AoI in TDMA considering the overhead is expressed as

$$\frac{1}{2N} \sum_{i=1}^{N} (k(n_i) + n_i + T_O)^2. \tag{5.4}$$

Finally, Fig. 5.5 shows the average AoI performance versus transmission probability in the slotted ALOHA with unit time slot $m = 1$ and transmission time slot $n_{\mathrm{SA},i} = m$, and as a benchmark, we show TDMA which considers the overhead can achieve the minimum AoI for $N = 4, 7$.

From Fig. 5.5(a), the slotted ALOHA with $N = 4$ can achieve a smaller average AoI as compared to the TDMA requiring $T_O \geq 5$. For example, if the amount of transmission data is 30 bits, it means that 150 bits are needed for allocation in TDMA. The overhead we have set is unrealistic, and we believe that the model would be more realistic if the required overhead were varied according to the system scale, such as the number of SNs. On the other hand, from Fig. 5.5(b), it can be seen that as the number of SNs increases, the average AoI of the slotted ALOHA increases more rapidly than TDMA, and slotted ALOHA with any transmission probability cannot achieve a smaller AoI than TDMA with overhead. Since all SNs in this study use the same transmission probability, the number of collisions increases with the increase in the number of SNs, and the average AoI is also expected to increase. In order to improve these results, each SN must determine its own transmission probability

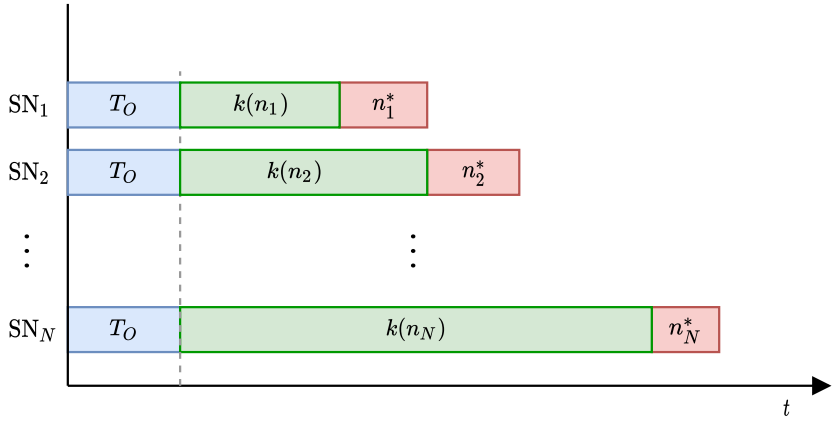


Fig. 5.4 Illustration of the allocation arrangements in the TDMA with overhead where $N$ SNs communicate with one FC.

according to the channel state, the amount of power harvested by EH, and the time since the system started.

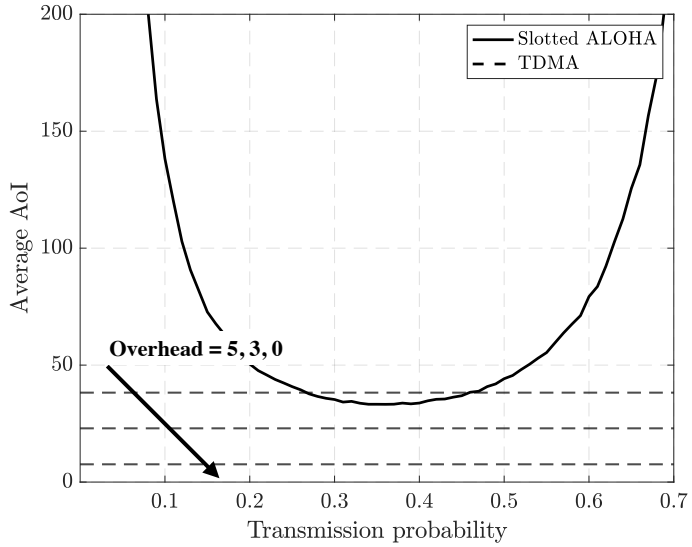


(a) Number of SNs: $N = 4$.

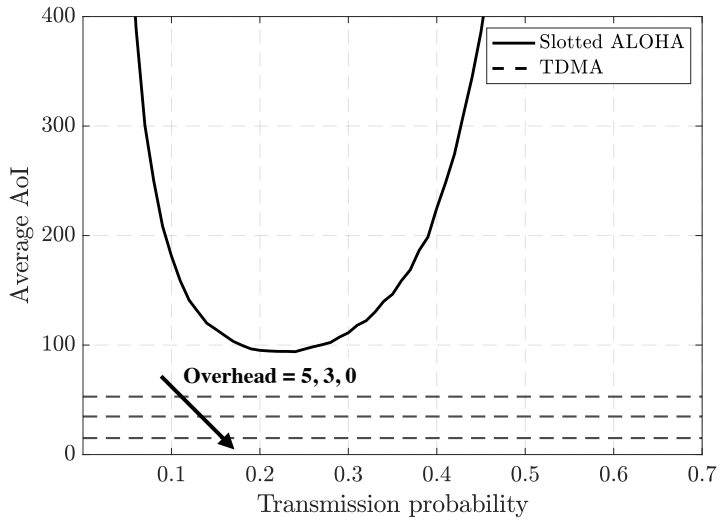


(b) Number of SNs: $N = 7$.

Fig. 5.5 Average AoI as a fuction of transmission probability in slotted ALOHA and TDMA with overhead.

# Chapter 6

# Conclusion

In this thesis, we considered the network where multiple SNs equipped with EH power supplies transmit their data to a common FC, aiming to create a maintenance-free wireless communications system.

Taking into account TDMA and FDMA as possible multiple-access schemes, we have reformulated the AoI minimization problems for both scenarios, analyzing their optimality conditions. Furthermore, we proposed novel resource allocation algorithms for these two schemes to solve the formulated optimization problems by leveraging the aforementioned analyses. We also discussed one of the basic random access scheme, the slotted ALOHA, and presented the formulation of the AoI and the process for data transmission. From the simulation results and previous study in [29], it is necessary to choose TDMA, FDMA or slotted ALOHA separately depending on available resources, size of the data packet, cost of overhead, and the time of packet observation in the system.

# Appendix A

# Proof of Proposition 1

In this appendix, we prove that equation (3.7) is convex with respect to the number of time slots $n$ assigned to a given SN by demonstrating that its second derivative is strictly positive under feasible parameter setups.

Indeed, differentiating equation $f(n)$ with respect to $n$ yields the first-order derivative as follows.

$$\frac{\mathrm{d}}{\mathrm{d}n} f(n) = g_1(n) \times g_2(n), \tag{A.1a}$$

with

$$g_1(n) \triangleq \frac{\beta n}{|h|^2}\left(2^{\frac{\gamma}{n}} - 1\right) + n, \tag{A.1b}$$

$$g_2(n) \triangleq \frac{\beta}{|h|^2}\left(2^{\frac{\gamma}{n}} - 1\right) - \frac{\beta}{|h|^2} 2^{\frac{\gamma}{n}} \log 2^{\frac{\gamma}{n}} + 1, \tag{A.1c}$$

where the auxiliary parameters $\beta \triangleq BN_0/E$ and $\gamma \triangleq D/B$ were introduced in order to simplify the expressions.

Next, taking the second derivative of $f(n)$ yields

$$\begin{aligned} \frac{\mathrm{d}^2 f(n)}{\mathrm{d}n^2} = \frac{\mathrm{d}}{\mathrm{d}n}(g_1(n) \times g_2(n)) = \overbrace{\big(g_2(n)\big)^2}^{\geq 0} \\ \times \left(\frac{\beta}{|h|^2}\big(\underbrace{2^{\frac{\gamma}{n}} - 1}_{\geq 0}\big) + 1\right) \frac{\beta}{|h|^2} 2^{\frac{\gamma}{n}} (\log 2^{\frac{\gamma}{n}})^2, \end{aligned} \tag{A.2}$$

where, since $\beta > 0$, $\gamma > 0$, $|h|^2 > 0$, $n > 0$, it follows that $\frac{\mathrm{d}^2 f(n)}{\mathrm{d}n^2} > 0$, completing the proof.

■

# Appendix B

# Proof of Proposition 2

Since $f(n)$ is a convex function with respect to $n$, it possesses a unique minimizer in $n \in [0,\infty)$ located at the point where its first-order derivative is equal to 0. In turn, as per equation (A.1), the minimizer of $f(n)$ must be a root of either $g_1(n)$ or $g_2(n)$, with the other bounded at that point.

Suffice it therefore to show that only the function $g_2(n)$ has a root in $n \in [0,\infty)$. To this end, let us first examine the following limits of $g_1(n)$

$$\lim_{n\to+0} g_1(n) = \lim_{n\to+0} \underbrace{\frac{\beta n}{|h|^2}\left(2^{\frac{\gamma}{n}}-1\right)}_{\to+\infty} + \underbrace{n}_{\to+0} = +\infty, \tag{B.1a}$$

$$\lim_{n\to+\infty} g_1(n) = \lim_{n\to+\infty} \underbrace{\frac{\beta n}{|h|^2}\left(2^{\frac{\gamma}{n}}-1\right)}_{\to+\infty} + \underbrace{n}_{\to+\infty} = +\infty, \tag{B.1b}$$

which combined with the fact that the term $(2^{\gamma/n}-1) \geq 0$, implies that $g_1(n)$ is strictly positive in $n \in \mathbb{R}$, and bounded within the interval limits.

Next, consider the limits of $g_2(n)$, namely

$$\begin{aligned} &\lim_{n\to+0} g_2(n) = \lim_{n\to+0} \frac{\beta}{|h|^2}\left(2^{\frac{\gamma}{n}}-1\right) - \frac{\beta}{|h|^2} 2^{\frac{\gamma}{n}} \log 2^{\frac{\gamma}{n}} + 1 \\ &= \lim_{n\to+0} \underbrace{\frac{\beta}{|h|^2} 2^{\frac{\gamma}{n}}}_{\to+\infty} \underbrace{\left(1-\log 2^{\frac{\gamma}{n}}\right)}_{\to-\infty} - \frac{\beta}{|h|^2} + 1 = -\infty, \end{aligned} \tag{B.2a}$$

and

$$\lim_{n\to+\infty} g_2(n) = \lim_{n\to+\infty} \frac{\beta}{|h|^2} \underbrace{\left[\left(2^{\frac{\gamma}{n}}-1\right)-2^{\frac{\gamma}{n}}\log 2^{\frac{\gamma}{n}}\right]}_{\to+0} + 1 = 1, \tag{B.2b}$$

which indicate that $g_2(n)$ possesses at least one root in the interval $n \in [0,\infty)$.

Finally, differentiating (A.1c) with respect to $n$ yields

$$\frac{\mathrm{d}}{\mathrm{d}n} g_2(n;h) = \frac{\beta\gamma^2\log^2(2)}{|h|^2 n^3} 2^{\frac{\gamma}{n}} > 0, \tag{B.3}$$

where the last inequality follows from the fact that for $E > 0$, $D > 0$, $B > 0$, $N_0 > 0$ and $|h|^2 > 0$, which in turn implies that $\beta \triangleq BN_0/E > 0$ and $\gamma \triangleq D/B > 0$.

Altogether, equations (B.2a), (B.2b) and (B.3) imply that the function $g_2(n;h)$ is monotonically increasing function from $-\infty$ to 1 and therefore has a single root in $n \in \mathbb{R}$, completing the proof. ■

# Appendix C

# Proof of Proposition 3

Our objective is to obtain upper and lower bounds to the solution of the equation

$$\overbrace{1-\frac{\beta}{|h|^2}+\frac{\beta}{|h|^2}\left(2-\log 2^{\frac{\gamma}{n}}\right)2^{\frac{\gamma}{n}}-\frac{\beta}{|h|^2}2^{\frac{\gamma}{n}}}^{g_2(n;h)\triangleq}=0, \tag{C.1}$$

where we have rewritten the function $g_2(n;h)$ defined in equation (A.1c), in a manner that will prove convenient in the sequel.

Next, consider the following bound

$$(2-\log 2^{\frac{\gamma}{n}})2^{\frac{\gamma}{n}}\leq e, \tag{C.2}$$

which is easily proved by defining $g_3(x)\triangleq(2-\log x)x$ with $x\triangleq 2^{\frac{\gamma}{n}}$ and observing that

$$\frac{\mathrm{d}}{\mathrm{d}x}g_3(x)\Big|_{x=e}=0, \tag{C.3a}$$

$$\frac{\mathrm{d}^2}{\mathrm{d}x^2}g_3(x)=-\frac{1}{x}<0,\ \forall x\geq 0, \tag{C.3b}$$

from which it follows immediately that the maximum value of $g_3(x)$ is achieved at the point $x=2^{\frac{\gamma}{n}}=e$, and given by

$$g_3(e)=(2-\log e)e=e. \tag{C.4}$$

Using inequality (C.2) in equation (C.1) readily yields the following functional upper bound to $g_2(n;h)$,

$$g_{2U}(n;h)\triangleq 1+\frac{\beta}{|h|^2}(e-1)-\frac{\beta}{|h|^2}2^{\frac{\gamma}{n}}. \tag{C.5}$$

It is obvious that the upper-bounding function $g_{2U}(n;h)$ is strictly ascending monotonic on $n$, such that due to the strictly ascending monotonicity of $g_2(n;h)$ itself, proved in Appendix B, it follows immediately that the root the $g_{2U}(n;h)$ is a lower bound on the root of $g_2(n;h)$, that is

$$g_{2U}(n_L;h)=0 \implies n_L^*=\frac{\gamma}{\log_2\left(\frac{|h|^2}{\beta}+e-1\right)}\leq n^*. \tag{C.6}$$

Finally, we note that at the point $2^{\frac{\gamma}{n}}=e$, where the equality $g_{2U}(n;h)=g_2(n;h)$ holds, we have

$$g_{2U}(n;h)=1-\frac{\beta}{|h|^2}>0,\ \forall\ |h|^2>\beta, \tag{C.7}$$

such that, again due to the monotonically ascending behaviors of both functions, it follows that as long as the condition $|h|^2>\beta$ is satisfied, we have

$$g_{2U}(n_U;h)=g_2(n_U;h) \implies n_U^*=\gamma\log 2\geq n^*, \tag{C.8}$$

which concludes the proof.

■

# Appendix D

# Proof of Proposition 4

Recall that the lower-bound $n_L^*$ on the optimal transmission time that minimizes the AoI of a given SN is the root of the upper-bounding function $g_{2U}(n;h)$, defined in equation (C.5), of the function $g_2(n;h)$, defined in equation (C.1).

Directly introducing the condition $|h_1|^2 > |h_2|^2$, and the equivalent relation $|h_2|^2 = |h_1|^2 - \eta$, with $\eta \in \mathbb{R}^+$, the difference between $g_{2U}(n;h_1)$ and $g_{2U}(n;h_2)$ yields

$$\begin{aligned} d(n;h_1,h_2) &\triangleq g_{2U}(n;h_1) - g_{2U}(n;h_2) \\ &= \frac{\eta\beta}{|h_1|^2|h_2|^2}\left(2^{\frac{\gamma}{n}} + 1 - e\right), \end{aligned} \tag{D.1}$$

which is obviously monotonically decreasing on $n$.

The latter fact, together with the trivial limits

$$\lim_{n\to+0} d(n;h_1,h_2) = +\infty, \tag{D.2a}$$

$$\lim_{n\to+\infty} d(n;h_1,h_2) = +0, \tag{D.2b}$$

implicates that $d(n;h_1,h_2) > 0$ in $n \in \mathbb{R}^+$, and consequently that $g_{2U}(n;h_1) > g_{2U}(n;h_2)$.

However, since $g_{2U}(n;h_1)$ and $g_{2U}(n;h_2)$ are themselves monotonically ascending functions, the above also implicates that the root $n_{1L}^*$ of $g_{2U}(n;h_1)$ is smaller than the root $n_{2L}^*$ of $g_{2U}(n;h_2)$, which proves inequality (3.17a).

Finally, we can observe from inequality (C.8) that the upper-bounding transmission time $n_U^*$ is independent of $|h|^2$, such that equation (3.17b) follows trivially, concluding the proof.

■

# Appendix E

# Proof of Proposition 5

Substituting the expression for the lower bound $n_L^*$ given in inequality (C.6) into equation (3.6) we have

$$k(n_L^*;h) = \frac{\gamma}{|h|^2}\frac{|h|^2+\beta(e-2)}{\log_2\left(\frac{|h|^2}{\beta}+e-1\right)}. \tag{E.1}$$

In order to prove implication (3.18a), it is sufficing to verify that for $|h_1|^2 > |h_2|^2 > \beta$

$$\begin{aligned}
&k(n_{2L}^*;h_2) - k(n_{1L}^*;h_1) \\
&= \frac{\gamma}{|h_2|^2}\frac{|h_2|^2+\beta(e-2)}{\log_2\left(\frac{|h_2|^2}{\beta}+e-1\right)} - \frac{\gamma}{|h_1|^2}\frac{|h_1|^2+\beta(e-2)}{\log_2\left(\frac{|h_1|^2}{\beta}+e-1\right)} \\
&= \underbrace{\frac{\gamma\log_2\left(\frac{|h_1|^2+\beta(e-1)}{|h_2|^2+\beta(e-1)}\right)}{\log_2\left(\frac{|h_1|^2}{\beta}+e-1\right)\log_2\left(\frac{|h_2|^2}{\beta}+e-1\right)}}_{\geq 0} + \frac{\beta\gamma(e-2)}{|h_1|^2|h_2|^2}\times \\
&\underbrace{\frac{|h_1|^2\log\left(\frac{|h_1|^2}{\beta}+e-1\right) - |h_2|^2\log\left(\frac{|h_2|^2}{\beta}+e-1\right)}{\log_2\left(\frac{|h_1|^2}{\beta}+e-1\right)\log_2\left(\frac{|h_2|^2}{\beta}+e-1\right)}}_{\geq 0} \geq 0.
\end{aligned} \tag{E.2}$$

In turn, substituting the expression for the upper bound $n_U^*$ given in inequality (C.8) into equation (3.6) yields

$$k(n_U^*;h) = \frac{\beta\gamma}{|h|^2}(e-1), \tag{E.3}$$

from what it follows trivially that $k(n^*_{1U};h_1) < k(n^*_{2L};h_2)$ for $|h_1|^2 > |h_2|^2$, which completes the proof.

■

# Appendix F

# Proof of Proposition 6

For convenience, let us first reproduce equations (3.15b) and (3.15d), namely

$$\bar{f}_B(n_1^*, n_2^*) = \frac{1}{2}\left(k(n_1^*) + n_1^*\right)^2 + \frac{1}{2}\left(k(n_1^*) + n_1^* + n_2^*\right)^2, \tag{F.1a}$$

$$\bar{f}_D(n_1^*, n_2^*) = \frac{1}{2}\left(k(n_2^*) + n_2^*\right)^2 + \frac{1}{2}\left(k(n_2^*) + n_2^* + n_1^*\right)^2, \tag{F.1b}$$

First, with respect to inequality (3.19a), it is readily found from these equations that

$$\begin{aligned} &\bar{f}_D(n_{1L}^*, n_{2L}^*) - \bar{f}_B(n_{1L}^*, n_{2L}^*) = \\ &\frac{1}{2}\left\{k(n_{2L}^*) + n_{2L}^*\right\}^2 + \frac{1}{2}\left\{k(n_{2L}^*) + n_{2L}^* + n_{1L}^*\right\}^2 \\ &-\frac{1}{2}\left\{k(n_{1L}^*) + n_{1L}^*\right\}^2 - \frac{1}{2}\left\{k(n_{1L}^*) + n_{1L}^* + n_{2L}^*\right\}^2 \geq 0, \end{aligned} \tag{F.2}$$

where the last inequality follows directly from inequality (3.17a) in Proposition 4 and inequality (3.18a) in Proposition 5.

As for inequality (3.19b), we again observe that

$$\begin{aligned} &\bar{f}_D(n_{1U}^*, n_{2U}^*) - \bar{f}_B(n_{1U}^*, n_{2U}^*) = \\ &\frac{1}{2}\left\{k(n_{2U}^*) + n_{2U}^*\right\}^2 + \frac{1}{2}\left\{k(n_{2U}^*) + n_{2U}^* + n_{1U}^*\right\}^2 \\ &-\frac{1}{2}\left\{k(n_{1U}^*) + n_{1U}^*\right\}^2 - \frac{1}{2}\left\{k(n_{1U}^*) + n_{1U}^* + n_{2U}^*\right\}^2 \geq 0, \end{aligned} \tag{F.3}$$

where the last inequality follows from equality (3.17b) in Proposition 4 and inequality (3.18b) in Proposition 5, concluding the proof.

■

# Appendix G

# Proof of Proposition 7

Differentiating $f(B_i|n_i)$, we obtain

$$\frac{\mathrm{d}}{\mathrm{d}B_i} f(B_i|n_i) = \left(\alpha_i B_i n_i \left(2^{\frac{D_i}{B_i n_i}} - 1\right) + n_i\right) \times \left(\alpha_i n_i \left(2^{\frac{D_i}{B_i n_i}} - 1\right) - \alpha_i 2^{\frac{D_i}{B_i n_i}} \log 2^{\frac{D_i}{B_i}}\right), \tag{G.1}$$

where we have implicitly defined $\alpha_i \triangleq N_0/|h_i|^2 E_i$.

In turn, the second derivative of $f(B_i|n_i)$ is

$$\frac{\mathrm{d}^2}{\mathrm{d}B_i^2} f(B_i|n_i) = \left(\alpha_i 2^{\frac{D_i}{Bn_i}} \left(n_i - \log 2^{\frac{D_i}{Bn_i}}\right) + \alpha_i n_i + 1\right)^2 \times \alpha_i 2^{\frac{D_i}{B_i n_i}} \log 2^{\frac{D_i}{B_i}} \left(\frac{2n_i}{B_i} + \log 2^{\frac{D_i}{B_i}}\right) \tag{G.2}$$

From the latter equation, it is evident that for $\alpha_i > 0$, $D_i > 0$, $n_i > 0$, $n_i > 0$, we have $\mathrm{d}^2 f(B_i|n_i)/\mathrm{d}B_i^2 > 0$, which indicates that $f(B_i|n_i)$ is strictly convex with respect to $B_i$ concluding the proof.

■

# References


[1] V. J. Hodge, S. O'Keefe, M. Weeks, and A. Moulds, "Wireless sensor networks for condition monitoring in the railway industry: A survey," *IEEE Trans. Intell. Transp. Syst.*, vol. 16, no. 3, pp. 1088–1106, Jun. 2015.

[2] A. B. Noel, A. Abdaoui, T. Elfouly, M. H. Ahmed, A. Badawy, and M. S. Shehata, "Structural health monitoring using wireless sensor networks: A comprehensive survey," *IEEE Commun. Surveys Tuts.*, vol. 19, no. 3, pp. 1403–1423, Apr. 2017.

[3] B. Maag, Z. Zhou, and L. Thiele, "A survey on sensor calibration in air pollution monitoring deployments," *IEEE Internet Things J.*, vol. 5, no. 6, pp. 4857–4870, Dec. 2018.

[4] Q. Qi and F. Tao, "Digital twin and big data towards smart manufacturing and industry 4.0: 360 degree comparison," *IEEE Access*, vol. 6, pp. 3585–3593, Jan. 2018.

[5] F. Tao, H. Zhang, A. Liu, and A. Y. C. Nee, "Digital twin in industry: State-of-the-art," *IEEE Trans. Ind. Inform.*, vol. 15, no. 4, pp. 2405–2415, Apr. 2019.

[6] S. Sudevalayam and P. Kulkarni, "Energy harvesting sensor nodes: Survey and implications," *IEEE Commun. Surv. Tut.*, vol. 13, no. 3, pp. 443–461, Jul. 2011.

[7] L. Liu, R. Zhang, and K. Chua, "Wireless information transfer with opportunistic energy harvesting," *IEEE Trans. Wireless Commun.*, vol. 12, no. 1, pp. 288–300, Dec. 2013.

[8] M. Piñuela, P. D. Mitcheson, and S. Lucyszyn, "Ambient RF energy harvesting in urban and semi-urban environments," *IEEE Trans. Microw. Theory Techn.*, vol. 61, no. 7, pp. 2715–2726, Jul. 2013.

[9] K. Sugiyama, H. Iimori, and G. T. F. de Abreu, "Statistical analysis of EH battery state under noisy energy arrivals," in *Proc. IEEE Int. Workshop Sig. Process. Adv. Wireless Commun. (SPAWC)*, Kalamata, Greece, Jun. 2018.

[10] T. Kawaguchi, R. Tanabe, R. Takitouge, K. Ishibashi, and K. Ishibashi, "Implementation of condition-aware receiver-initiated mac protocol to realize energy-harvesting wireless sensor networks," in *Proc. 2018 15th IEEE Annu, Consum. Commun. Netw. Conf. (CCNC)*, Jan. 2018, pp. 1–3.

[11] S. Sarma and K. Ishibashi, "Time-to-recharge analysis for energy-relay-assisted energy harvesting," *IEEE Access*, vol. 7, pp. 139 924–139 937, Sep. 2019.

[12] S. Ulukus, A. Yener, E. Erkip, O. Simeone, M. Zorzi, P. Grover, and K. Huang, "Energy harvesting wireless communications: A review of recent advances," *IEEE J. Sel. Areas Commun.*, vol. 33, no. 3, pp. 360–381, Mar. 2015.

[13] E. Uysal-Biyikoglu, B. Prabhakar, and A. El Gamal, "Energy-efficient packet transmission over a wireless link," *IEEE/ACM Trans. Netw.*, vol. 10, no. 4, pp. 487–499, Aug. 2002.

[14] J. A. Paradiso and T. Starner, "Energy scavenging for mobile and wireless electronics," *IEEE Pervasive Comput.*, vol. 4, no. 1, pp. 18–27, Jan. 2005.

[15] J. Yang and S. Ulukus, "Optimal packet scheduling in a multiple access channel with energy harvesting transmitters," *J. Commun. Netw.*, vol. 14, no. 2, pp. 140–150, Apr. 2012.

[16] H. Kawabata, K. Ishibashi, S. Vuppala, and G. T. F. de Abreu, "Robust relay selection for large-scale energy-harvesting IoT networks," *IEEE Internet Things J.*, vol. 4, no. 2, pp. 384–392, Jun. 2017.

[17] R. Tanabe, T. Kawaguchi, R. Takitoge, K. Ishibashi, and K. Ishibashi, "Energy-aware receiver-driven medium access control protocol for wireless energy-harvesting sensor networks," in *Proc. 2018 15th IEEE Annual Consum. Commun. Netw. Conf. (CCNC)*, Jan. 2018, pp. 1–6.

[18] S. Kahrobaee and M. C. Vuran, "Vibration energy harvesting for wireless underground sensor networks," in *Proc. 2013 IEEE Intern. Conf. Commun. (ICC)*, Jun. 2013, pp. 1543–1548.

[19] S. Kaul, M. Gruteser, V. Rai, and J. Kenney, "Minimizing age of information in vehicular networks," in *Proc. IEEE Sensor, Mesh Ad Hoc Commun. Netw. (SECON)*, Jun. 2011, pp. 350–358.

[20] S. Kaul, R. Yates, and M. Gruteser, "Real-time status: How often should one update?" in *Proc. IEEE INFOCOM*, Mar. 2012, pp. 2731–2735.

[21] R. D. Yates and S. K. Kaul, "The age of information: Real-time status updating by multiple sources," *IEEE Trans. Inf. Theory*, vol. 20, pp. 1807–1827, Mar. 2018.

[22] M. Costa, M. Codreanu, and A. Ephremides, "Age of information with packet management," in *Proc. IEEE Int. Symp. Inf. Theory (ISIT)*, Jun. 2014, pp. 1583–1587.

[23] B. Buyukates, A. Soysal, and S. Ulukus, "Age of information in multicast networks with multiple update streams," in *Proc. Asilomar Conf. Sign. Syst. Comput.*, Nov. 2019, pp. 1977–1981.

[24] A. Maatouk, S. Kriouile, M. Assaad, and A. Ephremides, "The age of incorrect information: A new performance metric for status updates," *IEEE/ACM Trans. Netw.*, pp. 1–14, Jul. 2020.

[25] E. Fountoulakis, N. Pappas, M. Codreanu, and A. Ephremides, "Optimal sampling cost in wireless networks with age of information constraints," in *Proc. IEEE Conf. Comput. Commun. Workshops (INFOCOM WKSHPS)*, Jul. 2020, pp. 918–923.

[26] Q. He, D. Yuan, and A. Ephremides, "Optimal link scheduling for age minimization in wireless systems," *IEEE Trans. Inf. Theory*, vol. 64, no. 7, pp. 5381–5394, Jul. 2018.

[27] T. Kuo, "Minimum age TDMA scheduling," in *Proc. IEEE INFOCOM*, Apr. 2019, pp. 2296–2304.

[28] A. Maatouk, M. Assaad, and A. Ephremides, "Minimizing the age of information: NOMA or OMA?" in *Proc. IEEE INFOCOM - IEEE Conf. Comput. Commun. Workshops (INFOCOM WKSHPS)*, Apr. 2019, pp. 102–108.

[29] H. Pan and S. C. Liew, "Information update: TDMA or FDMA?" *IEEE Wireless Commun. Lett.*, vol. 9, no. 6, pp. 856–860, Jun. 2020.

[30] P. R. Jhunjhunwala, B. Sombabu, and S. Moharir, "Optimal AoI-aware scheduling and cycles in graphs," *IEEE Trans. Commun.*, vol. 68, no. 3, pp. 1593–1603, Mar. 2020.

[31] A. Kosta, N. Pappas, A. Ephremides, and V. Angelakis, "Age of information performance of multiaccess strategies with packet management," *J. Commun. Netw.*, vol. 21, no. 3, pp. 244–255, Jun. 2019.

[32] A. Maatouk, M. Assaad, and A. Ephremides, "On the age of information in a csma environment," *IEEE/ACM Trans. Netw.*, vol. 28, no. 2, pp. 818–831, Apl. 2020.

[33] X. Wu, J. Yang, and J. Wu, "Optimal status update for age of information minimization with an energy harvesting source," *IEEE Trans. Green Commun. Netw.*, vol. 2, no. 1, pp. 193–204, Mar. 2018.

[34] B. T. Bacinoglu, Y. Sun, E. Uysal–Bivikoglu, and V. Mutlu, "Achieving the age-energy tradeoff with a finite-battery energy harvesting source," in *Proc. IEEE Intern. Symp. Inform. Theory (ISIT)*, Jun. 2018, pp. 876–880.

[35] A. Arafa, J. Yang, S. Ulukus, and H. V. Poor, "Online timely status updates with erasures for energy harvesting sensors," in *Proc. ALLERTON*, Oct. 2018, pp. 966–972.

[36] Y. Dong, P. Fan, and K. B. Letaief, "Energy harvesting powered sensing in iot: Timeliness versus distortion," *[Online]. Available:arXiv:1912.12427*, 2019.

[37] A. Arafa, J. Yang, S. Ulukus, and H. V. Poor, "Age-minimal transmission for energy harvesting sensors with finite batteries: Online policies," *IEEE Trans. Inform. Theory*, vol. 66, no. 1, pp. 534–556, Jan. 2020.

[38] Z. Chen, N. Pappas, E. Björnson, and E. G. Larsson, "Age of information in a multiple access channel with heterogeneous traffic and an energy harvesting node," in *Proc. IEEE Conf. Comput. Commun. Workshops (INFOCOM WKSHPS)*, Apl. 2019, pp. 662–667.

[39] T. Hara and K. Ishibashi, "Grant-free non-orthogonal multiple access with multiple-antenna base station and its efficient receiver design," *IEEE Access*, vol. 7, pp. 175 717–175 726, Nov. 2019.

[40] S. Ogata, K. Ishibashi, and G. T. F. de Abreu, "Optimized frameless aloha for cooperative base stations with overlapped coverage areas," *IEEE Trans. Wireless Commun.*, vol. 17, no. 11, pp. 7486–7499, Sep. 2018.

[41] *Performance datasheet of the vibration energy harvesters*, ReVibe Energy. [Online]. Available: https://revibeenergy.com/wp-content/uploads/2020/03/ReVibeEnergy_General.pdf

[42] V. Gupta and S. De, "Adaptive multi-sensing in eh-wsn for smart environment," in *Proc. 2019 IEEE Global Commun. Conf. (GLOBECOM)*, Dec. 2019, pp. 1–6.

[43] V. Naware, G. Mergen, and L. Tong, "Stability and delay of finite-user slotted aloha with multipacket reception," *IEEE Trans. Inform. Theory*, vol. 51, no. 7, pp. 2636–2656, Jul. 2005.

[44] S. Boyd, N. Parikh, E. Chu, B. Peleato, and J. Eckstein, "Distributed optimization and statistical learning via the alternating direction method of multipliers," *Found. Trends Mach. Learn.*, vol. 3, no. 1, pp. 1–122, Jan. 2011.

[45] R.-A. Stoica, H. Iimori, G. T. F. de Abreu, and K. Ishibashi, "Frame theory and fractional programming for sparse recovery-based mmwave channel estimation," *IEEE Access*, vol. 7, pp. 150 757–150 774, Oct. 2019.

[46] S. Kurt and B. Tavli, "Path-loss modeling for wireless sensor networks: A review of models and comparative evaluations." *IEEE Antennas Propag. Mag.*, vol. 59, no. 1, pp. 18–37, Jan. 2017.

# Publications

## Journal Paper

1. Naoya Hirosawa, Hiroki Iimori, Koji Ishibashi and Giuseppe Thadeu Freitas de Abreu, "Minimizing Age of Information in Energy Harvesting Wireless Sensor Networks," *IEEE Access*, vol. 8, pp. 219934-219945, Nov. 2020.

## International Conference Paper

1. Naoya Hirosawa, Hiroki Iimori, Giuseppe Thadeu Freitas de Abreu and Koji Ishibashi, "Age-of-Information Minimization in Two-User Multiple Access Channel with Energy Harvesting," in *Proc. CAMSAP2019*, pp.361-pp.365, Guadeloupe, French West Indies, Dec. 2019.

## Domestic Conference Papers

1. Naoya Hirosawa, Hiroki Iimori, Giuseppe Thadeu Freitas de Abreu and Koji Ishibashi, "A Study on Age-of-Information of Slotted ALOHA with Energy Harvesting," *IEICE General Conference 2021*, Mar. 2021 (submitted).

2. Naoya Hirosawa, Hiroki Iimori, Koji Ishibashi and Giuseppe Thadeu Freitas de Abreu, "Optimal Transmission Strategy Realizing Minimum Age-of-Information of Energy Harvesting Users over Multiple-Access Channels ," *IEICE Tech. Rep.*, vol. 120, no. 10, RCS2020-8, pp. 43–48, Apr. 2020.

3. Naoya Hirosawa and Koji Ishibashi, "A Study on Age-of-Information Minimization in Two-User Multiple Access Channel with Energy Harvesting," *IEICE Tech. Rep.*, vol. 119, no. 90, RCS2019-88, pp. 297–302, Jun. 2019.